universität wien

MASTERARBEIT

Titel der Masterarbeit

„UNDERSTANDING SHARPIN'S ROLE IN REGULATION OF APOPTOSIS SIGNALLING IN VIVO“

>Band 1 von 5 Bänden<

Verfasst von

Stefan Lutzmayer, BSc

angestrebter akademischer Grad

Master of Science (MSc)

Wien, 2014

Studienkennzahl lt. Studienblatt:	A 066 834
Studienrichtung lt. Studienblatt:	Masterstudium Molekulare Biologie
Betreut von:	Fumiyo Ikeda, PhD

Table of contents

Introduction

Ubiquitin

Possible functionality of mammalian proteins can be extensively modulated by posttranslational modifications[1]. Besides attachment of phosphate, methyl or acetyl residues, entire proteins, such as Ub, can be attached on substrates[2]. Ub, first described in 1980[3] for targeting substrates to the proteasome is extensively studied till today and is known to regulate diverse cellular processes including regulation of transcription, DNA repair, ribosomal function, cell cycle, and signalling, most notably in Nf-κB[4-8].

The ubiquitously expressed polypeptide Ub consists of 76-amino acid residues and is highly conserved underlining its essential role amongst species[9,10]. Ub covalently modifies substrates, most commonly on lysine residues[11]. It is a highly stable protein that contains a β-grasp fold, hydrophobic patches on the surface and a very flexible C-terminal tail structure[12]. Ubiquitinated substrates are decoded by enzymes possessing Ub binding domains (UBDs) which in most cases recognise the Ub's hydrophobic patches[13].

Ubiquitin system

Linking Ub onto the substrate is achieved by a three-step enzymatic reaction resulting in an isopeptide bond between the ε-amino group of the substrate or another Ub molecule and the C-terminal glycine of Ub[2]. In the first step, Ub is activated in an ATP dependent manner using the E1 Ub activating enzyme (Figure 1). Activated Ub-AMP intermediate then acts as a donor for a cysteine residue in the active site of E1, which removes AMP and forms a high-energy thioester bond[14]. Subsequently, Ub is transferred from E1's cysteine to the active-site cysteine of an E2 Ub-conjugating enzyme – by transthiolation (Figure 1)[15,16]. Finally, the Ub is attached on the substrate by an E3 ligase (Figure 1)[17]. The human genome encodes only two Ub E1s, 38 Ub E2s and over 600 Ub E3 ligases[18]. Ubiquitination is a reversible process, the removal is carried out by deubiq-

uitinating enzymes (DUBs) that cleave off Ub, in either linkage or substrate specific manner, which gets recycled and can be reused[19].

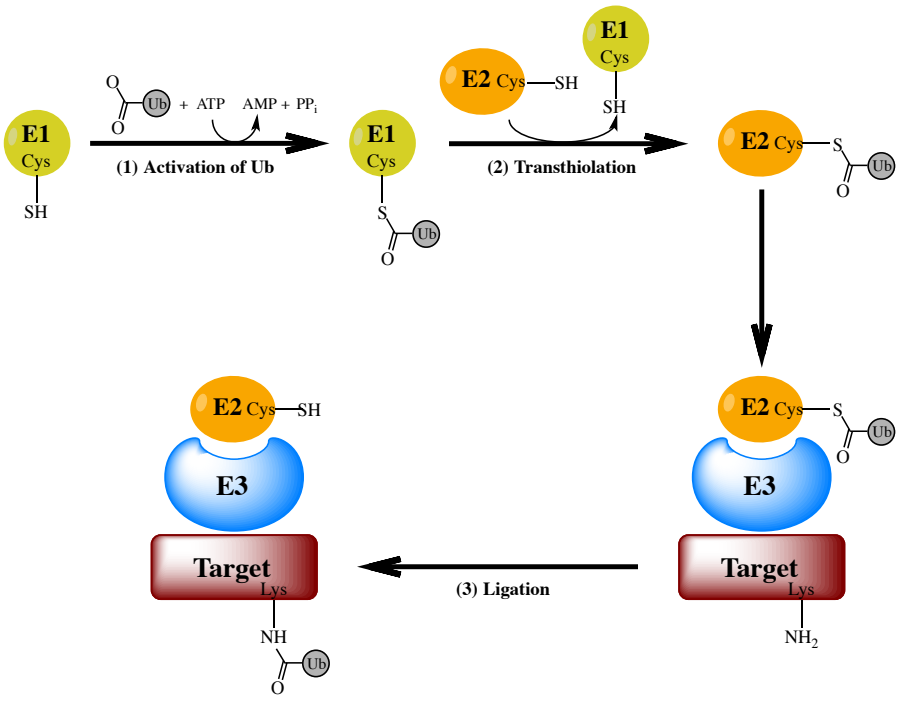

Figure 1 | The Ub system. (1) ATP dependent activation of Ub and transfer on E1 (thioesther bond). **(2)** Transfer of Ub moiety from E1 onto active cysteine of E2 via transthiolation. **(3)** Ligation of the Ub from the E2 on the target lysine residue of the substrate resulting in an isopeptide bond. Ub: Ub, Lys: lysine, Cys: cystein

Ubiquitination can be classified in three different types: mono-ubiquitination, where a single Ub molecule is attached to a lysine residue of the substrate; multi-mono-ubiquitination, when several Lysine residues on a substrate are modified; and poly-ubiquitination, if a Ub polymere is added[5]. Since Ub itself possess seven internal lysine (Lys) residues (Lys6, Lys11, Lys27, Lys29, Lys33, Lys48, and Lys63), which can be utilised for ubiquitination, it is possible to form Ub chains in various length and three-dimensional topology depending on the linkage types[5]. Furthermore, a novel type of poly-Ub chains, linear-Ub (lin-Ub) chains has been discovered[20]. The C-terminal Glycine 76 of a donor Ub is linked to the α-amino group of methionine 1 of the acceptor Ub creating a peptide bond resulting in a head-to-tail or lin-Ub linkage[20]. These eight different

Ub chain types, using either one of the seven Lys residues or the amino terminal methionine 1, achieve the great variety of physiological roles of Ub modification[21]. Amongst those, Lys48 and Lys63 linked Ub chains have been investigated intensively; much less is known about the other 'atypical' Ub chains[22].

E1 activating enzymes

E1 enzymes are responsible for the initiation of the conjugation cascade for each Ub or Ub like enzyme (Ubl)[23]. Ub C-terminal glycine is adenylated by ATP hydrolyses and the release of PP_i (Figure 1). After this intermediate step, Ub is linked via a thioester bond to the active site cysteine of the E1 and AMP is released (Figure 1). Fully loaded E1 enzymes carry two Ub molecules, one bound as an adenylate intermediate that serves as a donor for the active site cysteine, and another bound as a thioester[24]. E1 enzymes are highly efficient and manage, even at lower concentrations than of E2s and E3s, to supply enough activated Ub moieties for the subsequent reactions to occur[14].

E2 conjugating enzymes

E2 enzymes accomplish to discriminate between Ubl and Ub loaded E1s by specifically recognising a binding site exposed at Ub loaded E1 molecules[24,25] and play an essential role in determining Ub chain topology and length[16]. A tight E1-E2 complex is formed, and Ub is transferred by transthiolation onto the catalytic cysteine of the E2 conjugating enzyme[16]. Subsequently, E1 is released from the complex and Ub loaded E2 can interact with a Ub E3 ligase (Figure 1)[26].

E3 Ligases

E3 ligases can be classified based on ligase function and structure into RING (really interesting new gene)-type E3 ligase[27], HECT (homologous to the E6AP carboxyl terminus)-type E3 ligase[28] and RING-HECT hybrids[29,30]. RING type E3 ligases are not catalytically active, instead they bring the substrate and the Ub-loaded E2 into close proximity and facilitate catalysis by exploiting E2's enzymatic activity (Figure 2A); thereby, the E2 defines the linkage specificity[31]. In contrast, HECT-type E3 ligases possess a catalytic cysteine and do not solely serve as bridging factors[32]. Ub gets transferred from E2 to a

cysteine on the HECT C-terminus and later onto the substrate[33] (Figure 2B); thus, they can define different linkage types utilising the same E2[32].

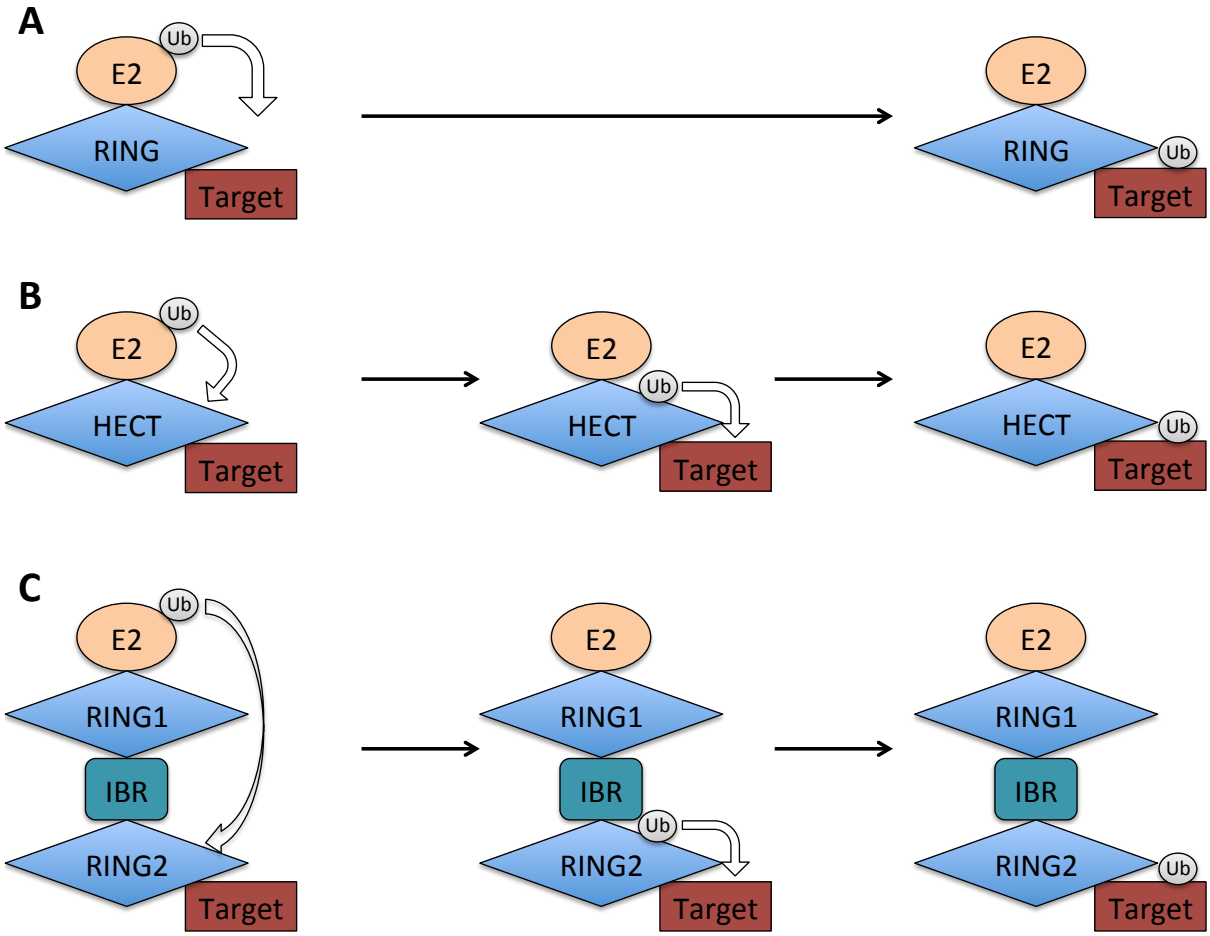

Figure 2| Model of Ub formation by RING, HECT and RBR type E3 ligases. A RING E3s convey proximity of the Ub loaded E2 and the substrate to enable direct transfer of the Ub onto the substrate. **B** HECT E3 function comprises a covalent Ub-E3 intermediate step and a subsequent transfer on the substrate. **C** A hybrid mechanism is employed by RBR E3s; first, the Ub loaded E2 is bound to RING1 and Ub is transferred to RING2 domain which catalyses substrate ubiquitination. Ub: Ub; RING: really interesting new gene; HECT: homologous of the E6AP carboxyl terminus; RBR: RING-between-RING, IBR: In-Between-RING finger.

Additionally, E3 ligases characterised by a sequence of RING, in-between-RING and RING domain called RBR-type E3 combine the features of RING and HECT-type E3s[29]. The RING1 domain binds Ub loaded E2 and bridges E2 dependent Ub transfer on the catalytic active cysteine on the RING2 domain that ubiquitinates the substrate using

its ligase activity[34] (Figure 2C). RBRs showed to define the linkage type independently of the respective E2 enzyme[35]. Members of the RBR family have been implicated in signalling cascades and pathological conditions[36-39]. Mutations in the RBR type E3 ligase parkin lead to defects in protein degradation; hence, proteins accumulate (Lewy body) and cause the autosomal recessive form of juvenile Parkinson disease[39]. Drosophila RBR Ariadne is essential for development as KO is embryonic lethal[40]. The human homolog HHARI is supposed to have redundant functions as parkin and could explain cell type specific differences in Parkinson's disease[41]. In addition, RBR family E3 ligase complex LUBAC was studied intensively and revealed crucial functions in e.g. Nf-κB activation, apoptosis regulation or osteogenesis[36,38,42-46].

LUBAC

LUBAC (linear Ub chain assembly complex) (Figure 3) is the only E3 ligase complex known to generate linear methionine 1 linked (M1-linked) Ub chains and it belongs to the RBR-type E3 ligases[20]. LUBAC is a large tripartite 600kDa complex consisting of the catalytic protein HOIP (HOIL-1L interacting protein) also known as RNF31/Zibra/PAUL, and two regulative subunits: HOIL-1L (Heme-oxidised iron-regulatory protein 2 Ub ligase 1L), and SHARPIN (SHANK associated RH domain-interacting protein), the latter of which was recently identified as third component of LUBAC[20,38,42,45]. LUBAC regulates Nf-κB activation by ubiquitinating the IKK complex regulatory subunit NEMO (Nf-κB essential modulator)[36,37]. Recently, the lin-Ub specific DUB OTULIN was shown to counteract LUBAC induced Nf-κB activation[47].

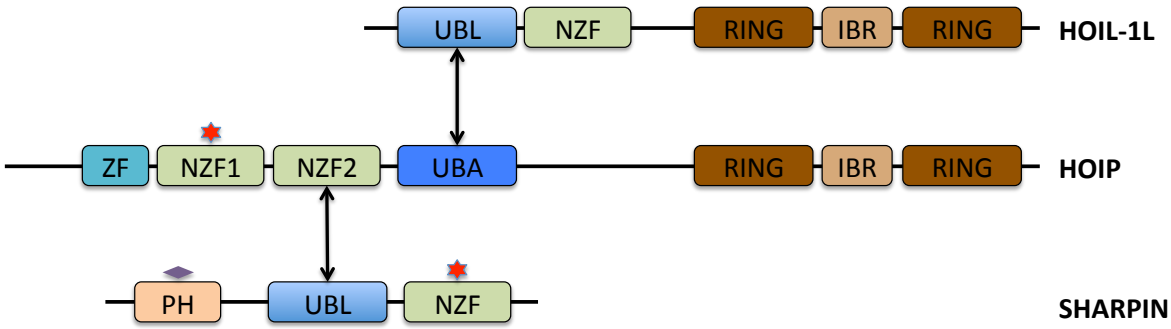

Figure 3 | LUBAC component domain architecture and interactions. HOIL-1L and SHARPIN interact with the catalytically active HOIP using their UBL domain, specifically interacting with HOIP's UBA and NZF2 domain respectively[20]. NZF domains in HOIL and SHARPIN as well as NZF1 domain in HOIP (indicated with stars) interact with Ub. SHARPIN's PH domain (indicated by the pink diamond) enables homodimer formation. Ub: Ub; LUBAC: linear Ub chain assembly complex; HOIL-1L: Heme-oxidised iron-regulatory protein 2 Ub ligase 1L; SHARPIN: SHANK associated RH domain-interacting protein; HOIP: HOIL-1L interacting protein; UBL: Ub like domain; NZF: Npl4-type zinc finger; UBA: Ub-associated domain; PH: pleckstrin homology domain

HOIP

HOIP is the catalytic active 120kDa protein of the LUBAC E3 ligase complex responsible for generating lin-Ub chains and was first identified as binding partner of the muscle specific kinase in the neuromuscular junction[48]. It features a N-terminal PUB domain (PNGase/Ub-associated) followed by three Ran-BP2-type zinc fingers (ZFs), a UBA domain (Ub-associated) and a C-terminal RBR domain (Figure 3)[20]. HOIP is auto-inhibited by its N-terminus, which is released after binding to either HOIL-1L or SHARPIN or both in combination[49]. The RBR domain is responsible for HOIP's ligase activity and discrimination towards M1-linked Ub chains by orienting the acceptor Ub methionine 1 α-amino group in close proximity to the catalytic centre[35].

HOIL-1L

HOIL-1L or RBCK1 is a regulatory 50kDa subunit of the LUBAC complex[20]. The shorter splice variant HOIL-1 was first described as an E3 ligase that recognises oxidised proteins[50,51]. RT-PCR analysis revealed that the longer splice variant HOIL-1L was more abundant and pull down experiments later identified a 600kDa complex that includes

HOIP[20]. Starting from the N-terminus, HOIL presents a UBL domain followed by one Npl4-type zinc finger (NZF) and an RBR domain (Figure 3)[20].

SHARPIN

SHARPIN, a 40kDa protein, was first found to associate with SHANK in the postsynaptic density of excitatory neurotransmitters in the brain[52] and in 2011 it was identified as the third component of LUBAC regulating apoptosis and Nf-κB activation[38,42,45]. Its N-terminus features a pleckstrin homology (PH) domain for dimerisation[52]. Furthermore, SHARPIN has high sequence similarity to the N-terminus of HOIL-1L and contains a UBL and an NZF domain (Figure 3)[53].

Seymour *et al* showed that spontaneous point deletion arising in the SHARPIN gene leads to a multisystem diseases called cpdm (chronic proliferative dermatitis in mice) at 3-5 weeks of age characterised by skin inflammation and multi-organ phenotype including splenomegaly, dermatitis and defects in secondary lymphoid organs[54]. Additionally, non-immunological organs like lung and liver show immune cell infiltrates, organised Peyer's patches in the small intestines are absent and spleen germinal centre formation is defective[55-57]. This single base pair deletion at the 3'-end of SHARPIN exon 1 on chromosome 15, results in a frame shift, causing an early stop codon and no functional protein product responsible for cpdm phenotype[54]. In contrast, genetic ablation of the second LUBAC regulatory subunit HOIL-1L, does not give an apparent phenotype[36,43].

SHARPIN KO mice from here on referred to as CPDM mice, suffer from severe epidermal skin lesions that present hyperkeratosis, hyperplasia and parakeratosis; the skin diseases resembles a human hereditary diseases called psoriasis[56]. The skin phenotype can be rescued in mice deficient for already one TNF allele whereas, multi-organ phenotype is not affected[42].

Intriguingly, keratinocytes in SHARPIN deficient mice show hyper upregulation of apoptosis via FADD and caspase-8 suggesting a possible connection between inflammation and cell-death[38,42,45]. Analysis of CPDM mice derived cells showed diminished levels

of canonical Nf-κB activation and an up-regulation of apoptosis after TNF-α stimulation[38,42,45].

The Nf-κB pathway

Nuclear factor kappa-light-chain-enhancer of activated B cells (Nf-κB) was discovered in B-cell tumours over 25 years ago and the underlying biological mechanisms have been intensively studied in the past decades[58]. The Nf-κB transcription factor (TF) family regulates a wide array of cellular processes including inflammation, cell survival, skeletal development or apoptosis[8,59,60]. The Nf-κB signalling is categorised into a canonical pathway, activated as a result of signalling events triggered by cytokines (e.g. TNF-α, IL-1β) or pathogen associated molecular patterns (PAMPs); and non-canonical pathways[61]. Dysregulations of the Nf-κB pathway have been linked to pathological conditions like cancer and autoimmune diseases[62,63]; hence, Nf-κB regulation is essential[63].

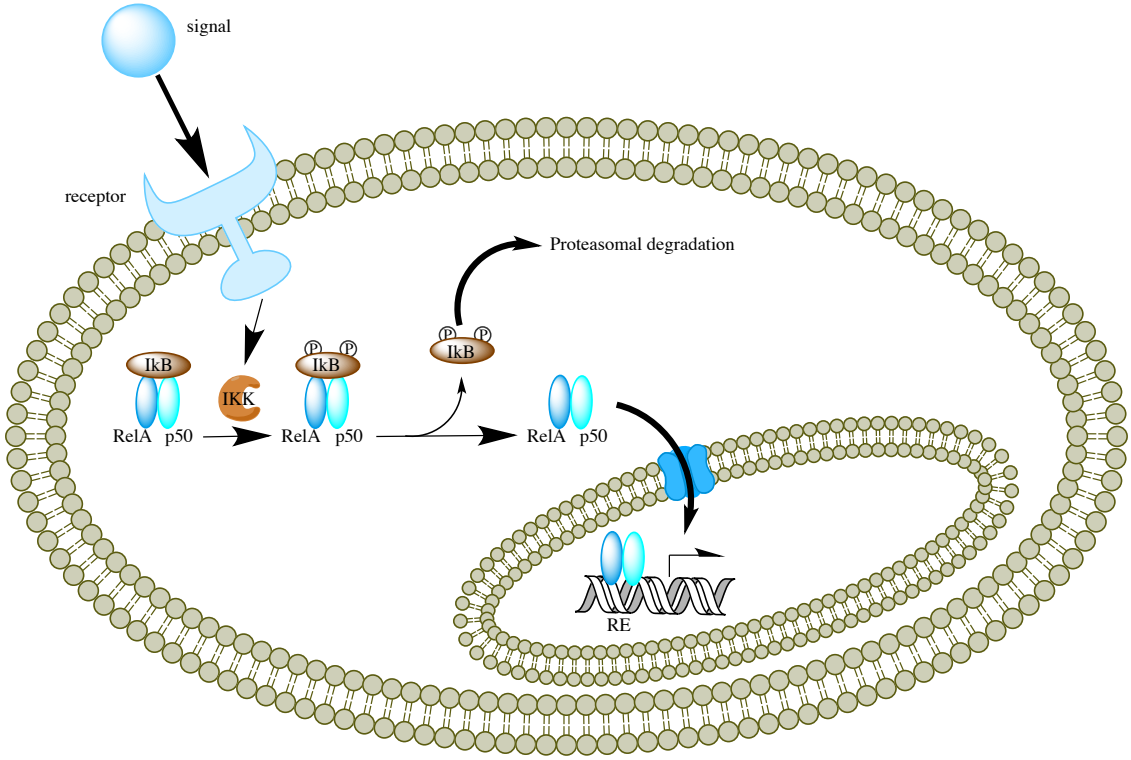

Figure 4 | Nf-κB schematic. Nf-κB TFs reside bound to IκB in the cytoplasm. Upon signal, IKK complex gets activated and phosphorylates IκB resulting in its degradation. Subsequently, Nf-κB translocates into the nucleus, binds to RE

and turns on target gene transcription. Nf-κB, Nuclear factor kappa-light-chain-enhancer of activated B cells B; TF, transcription factor; IκB, nuclear factor of kappa light polypeptide gene enhancer in B-cells inhibitor; IKK, IκB kinase; RE, response element

Under steady-state conditions, Nf-κB is bound to nuclear factor of kappa light polypeptide gene enhancer in B-cells inhibitor (IκBs) in a complex, which blocks the Nf-κB nuclear localisation signal (NLS)[64]. Upon stimulation, the inhibitors get phosphorylated by the IκB kinase complex (IKK), consisting of two kinases IKKα & IKKβ as well as the regulatory subunit NEMO (IKKɣ), and subsequently get degraded by the proteasome[65]; thus, Nf-κB's NLS is uncovered and it can translocate to the nucleus to activate target gene transcription (Figure 4)[61].

Nf-κB family members

Members of the Nf-κB superfamily (RelA (p65), RelB, c-Rel, p105/p50, p100/p52 & Relish) share similar domain architecture: They possess the Rel homology domain for homo-/heterodimerisation and IκB binding as well as a DNA binding domain[66]. RelA (p65), RelB and c-Rel utilise a transactivation domain located at their C-terminus to trigger gene expression upon DNA binding[67].

Nf-κB signalling through TNF receptor 1

Canonical Nf-κB activation can be achieved by several stimuli, including ligand binding to the tumour necrosis factor receptor 1 (TNFR1) that in addition to Nf-κB's pro survival function, is also capable of apoptosis induction through the death induced signalling complex (DISC)[68]. TNFR1 signalling is initiated when TNF-α binds to its extracellular component and results in receptor trimerisiation[69]. Subsequently, intracellular TNFR1 death domain (DD) is reorganised, leads to recruitment of TNFR1 associated death domain protein (TRADD) and receptor interacting protein 1 (RIP1)[70,71]. TNFR associated factor 2/5 (TRAF2/5) bind to TRADD, which leads to E3 ligase cellular inhibitor of apoptosis 1/2 (cIAP1/2) binding[72]. cIAP1/2 mediated RIP1 ubiquitination creates interaction sites for transforming growth factor-β activated kinase 1 (TAK1) / TAK1 binding protein (TAB) and IKK complex[73]. Subsequently, the formed multi-subunit cyto-

solic TNF receptor complex (TNF-RC) triggers mitogen activated protein kinase (MAPK) and Nf-κB pathway[74-76].

TNFR1 induced apoptosis requires the time dependent dissociation of TRADD, TRAF2/5 and RIP from the TNF-RC and recruitment of Fas associated protein with DD (FADD) and caspase-8 forming the DISC and initiate caspase cascade[77]. At physiological levels, Nf-κB induced gene expression results in inhibition of the caspase cascade through activation of anti-apoptotic protein gene expression, like cellular FLICE-like inhibitory protein (cFLIP)[78]. If Nf-κB activity is reduced, cellular responses switch from survival towards cell-death initiation[79].

LUBAC mediated linear ubiquitination in the TNF-RC

Various different Ub chain types are essential in Nf-κB regulation[80]. The TNF-RC is ubiquitinated by cIAPs to recruit TAK1/TAB and the LUBAC complex that generates lin-Ub chains in RIP1 and IKK component NEMO[43]. Subsequently, IKK phosphorylates IκBs, which leads to its Lys48-linked Ub-chain modification and proteasomal degradation (Figure 5)[80,81]. Besides Lys63 and lin-Ub chains, Lys11 poly-Ub chains in the TNF-RC might be important in bringing LUBAC to the receptor complex[82]. LUBAC was found to positively regulate TNF-RC mediated Nf-κB activation by binding and ubiquitinating NEMO and RIP1[36,43,44]; thereby, the IKK complex gets recruited to the TNF-RC through the highly specific lin-Ub binding domain in NEMO termed UBAN (Ub binding in ABIN and NEMO proteins)[44,83,84]. LUBAC is crucial in the TNF-RC, illustrated by the fact that genetic ablation of regulatory LUBAC component leads to reduced Nf-κB activation[38,42,85].

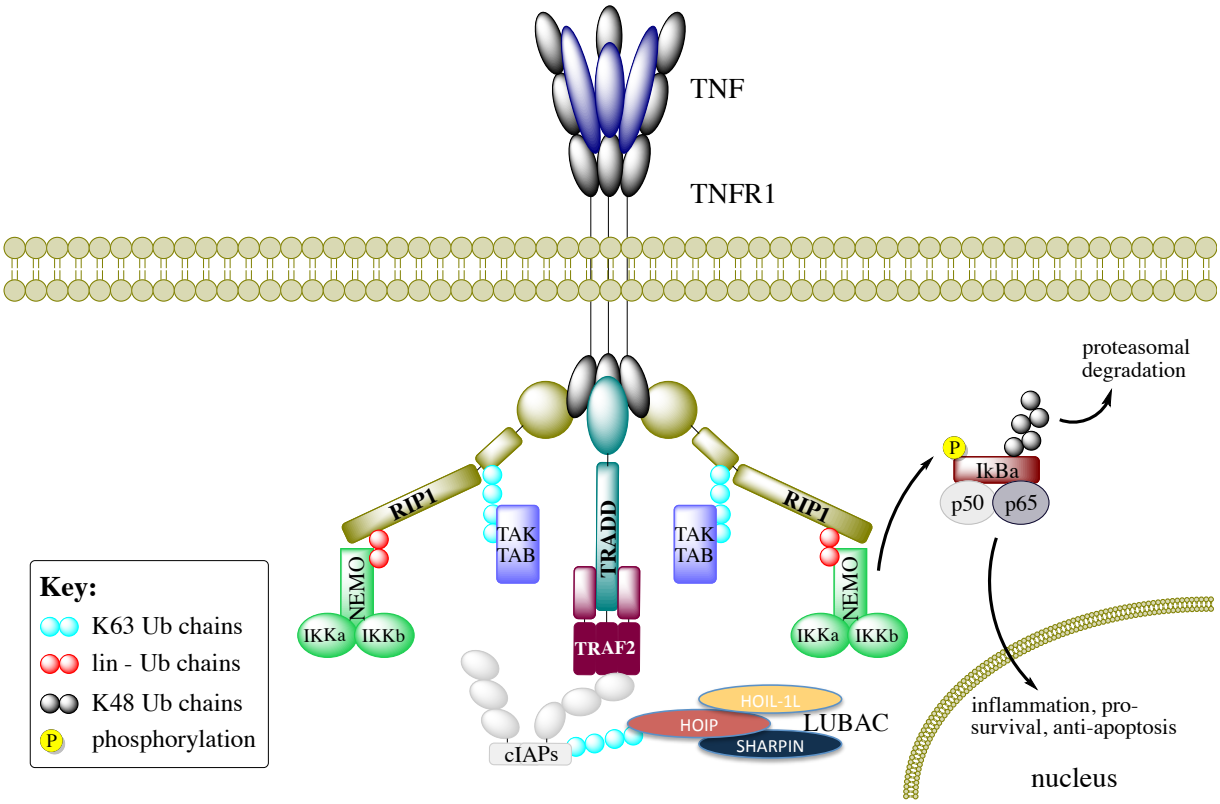

Figure 5 | The TNF-RC activates the canonical Nf-κB pathway. TNFR1 trimerises upon TNF binding, recruits TRADD and RIP1 via their DDs. TRAF2 binds to TRADD and recruits cIAPs E3 ligases, which put Lys63 linked Ub-chains on RIP1, which in turn brings the TAK/TAB and LUBAC complex to the TNF-RC. cIAPs are required to bring LUBAC to the complex, linearly ubiquitinating NEMO and RIP1. IKK binds to lin-Ub chains through NEMO's UBAN domain, phosphorylates IκBα that gets Lys48 ubiquitinated and degraded by the proteasome releasing p50/p65 to translocate to the nucleus and activating Nf-κB target gene expression. TNF-RC: tumour necrosis factor 1 receptor complex; TRADD: TNFR1 associated death domain protein; RIP1: receptor interacting protein 1; DD: death domain; TRAF2: TNFR associated factor 2; cIAP: cellular inhibitor of apoptosis; NEMO: Nf-κB essential modulator; TAK: transforming growth factor-β activated kinase; TAB: TAK1 binding protein; LUBAC: linear Ub chain assembly complex; IκB: nuclear factor of kappa light polypeptide gene enhancer in B-cells inhibitor IKK: IκB kinase; UBAN: Ub binding in abin1 and NEMO;

Mouse skin architecture

The skin is the largest organ, functions as first physical barrier protecting against pathogens and thereby is also important part of the immune system[86]. This is in addition to its other functions including temperature regulation, ultraviolet light protection, sensory functions and providing stability against mechanical stress[87]. Throughout the body, the skin is homogenously defined with some exceptions around eyes, mouth, anus and other body cavities. Nevertheless, the basic skin layer architecture is uniform (Figure 6). The outermost layer of the skin is the epidermis, which is attached to basal membrane through hemidesmosomes[88]. This membrane zone separates dermis from epidermis. Basal keratinocytes mediate the epidermis' structural integrity and furthermore provide the cell population for the epidermis by proliferating into more differentiated cells, migrate upwards towards the skin surface where they form the stratified skin surface[89]. The intermediate filament keratin is the major component of the epidermis; throughout differentiation of basal keratinocytes, different keratin variants are expressed and can be used to define epidermal layers[90]. Hair follicles are specialised form of keratin and associated proteins that are forming cell layers starting from invaginated epithelial buds[91].

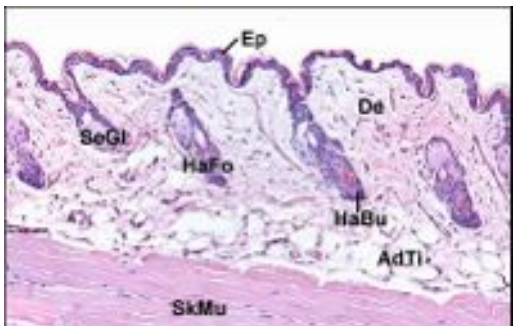

Figure 6 | Mouse skin layers. External epidermis (Ep), connective tissue layer dermis (De), Adipose tissue (AdTi), Hair bulp (HaBu), Hair follicle (HaFo), Skeletal muscle (SkMu), Sebaccous gland (SeGl). Adapted from http:// http://ctrgenpath.net.

Below the basement membrane, connective tissue composed of collagen fibres, elastic fibres, and extra fibrillar matrices forms the dermis[87]. Fibroblast are the most abundant cell type in the dermis; additionally, macrophages rest in the dermis in order to immediately react to pathogens[86]. Adipose tissue below the dermis hydrates the skin and provides connection to the lymphatic system[87]. Moreover, sweat and sebaceous glands are found in the dermis regulating temperature and to lubricate as well as hydrate the skin respectively[92,93].

Skin inflammation and Nf-κB

The skin represents the first barrier against harmful events, either pathogens or injuries[86]. When the skin is breached the complicated biological process of inflammatory response that can also affect internal organs and tissues is activated[94]. Resident innate immune cells, mostly macrophages, express surface receptors capable of recognising viruses, bacteria and parasites and trigger appropriate cytokine production and further targeted immune reactions[95]. Depending on the signal, typical skin inflammation induces blood vessel dilation, swelling and inflammatory pain resulting in typical skin reddening; hence, immune cells can more easily reach the target tissue[96]. Nf-κB is an essential regulator for inflammatory responses, up-regulating pro-inflammatory cytokine expression e.g. TNF-α, IL-1, IL-6 & IL-8 and enhances adhesive surface marker expression for enhanced neutrophils, macrophage and leukocyte recruitment respectively[97]. Acute inflammation resolves after clearance of the pathogen; if not, chronic inflammation or tumour formation may arise[98]. Pro-inflammatory cytokines have limited half-life and inflammatory cells undergo apoptosis[99]. In addition, anti-inflammatory cytokines are produced to control the process and retain tissue homeostasis[100]. Detailed mechanisms for inflammatory response clearance remain elusive demanding further research to disentangle the vital nods in the inflammatory signalling network[101].

Apoptosis a specialised form of programmed cell-death

Multicellular organisms depend on the vital process of controlled programmed cell-death (PCD) termed apoptosis for developmental processes and to maintain tissue steady-state conditions; furthermore, it is implicated in many disease conditions and cancer[102,103]. The hallmarks of apoptotic cells are fragmentation of the DNA and nuclear envelope breakdown, collapse of the cytoskeleton and exposure of surface markers on the cell for rapid removal by phagocytosis[104]. Upon intracellular or extracellular stimulation, cells undergo clearly defined and controlled programmed cell-death (apoptosis) opposed to detrimental necrosis[102]. Whilst, in necrosis the cell membrane is ruptured

and cytoplasmic components are released resulting in an inflammatory reaction[102]. In contrast, apoptotic cells are quickly and efficiently phagocytosed[105].

Signalling events that trigger apoptosis in mammalian cells have been well described and include intracellular and extracellular triggers[106]. Apoptosis relies on a special class of aspartic acid proteases termed caspases[107]. Those proteases are initially inactive precursors that need to be cleaved to become catalytically active[108]. So-called initiator caspases form multimeres or complexes with adapter proteins for auto-cleavage and consequently proteolytically cleave many downstream caspases amplifying the signal[107]. Next, effector caspases target non-caspase proteins and trigger the described hallmarks of apoptosis[109].

Lack of growth promoting factors or nutrients or apoptotic proteins can trigger changes in the mitochondrial membrane and thereby release of pro-apoptotic proteins, most commonly cytochrome c, into the cytoplasm[110]. Subsequently, the apoptosome is formed and initiates PCD[111]. Alternatively, extracellular stimuli can trigger apoptosis signalling after respective receptor binding; amongst those, TNF-α and Fas Ligand (FasL) signal propagation through the TNF-RC and Fas-receptor are best described[112,113]. Death domain containing protein FADD binds directly to Fas-receptor and to adaptor TRADD downstream of TNF signalling. Pro-caspase-8 gets recruited, activated and triggers downstream caspase cascade[107]. Cytotoxix T-cells (CTLs) can trigger apoptosis by FasL and Fas-receptor binding or perforation of the target cell membrane through perforines, resulting in transfer of granzymes, which are serine proteases that cleave initiator caspase-10[114].

Programmed cell-death needs to be tightly regulated, either by expression of anti-apoptotic proteins or inhibiting pro-apoptotic factors[115]. The Bcl-2 protein family enhances mitochondrial membrane integrity and thereby blocks cytochrome-c release[116]. Flip proteins bind to FADD and caspase-8, thereby forming an apoptosis inhibitory complex and block death induced signalling complex formation[78,117].

Aim of this work

Ubiquitination is essential in various biological processes. Recent studies showed, that besides typical Lys11-, Lys48- & Lys63-linked Ub chains also lin-Ub chains are involved in Nf-κB activation and apoptosis control[81]. Hence, further investigations are needed to clarify the precise regulatory mechanisms. Particularly, focusing on the possible connection between skin inflammation and apoptosis as seen in CPDM mice[38,42,45,118].

The aim of this thesis is to understand the phenotype of the non-catalytic LUBAC component SHARPIN by generating a double knockout mutant mouse line. SHARPIN mutant mice exhibit chronic skin inflammation as well as a multi-organ phenotype characterised by splenomegaly, eosinophilia, defects in secondary lymphoid organs and more[54-57,119]. SHARPIN is known to regulate inflammation and protect against TNF-α induced FADD/caspase-8 mediated apoptosis as CPDM mice showed enhanced levels of apoptosis in keratinocytes[38,42]. Together with in vitro biochemistry data (not published), we hypothesised that SHARPIN has specific interaction partners in TNF-α induced cell-death, which are ubiquitinated by LUBAC and trigger anti-apoptotic responses (Figure 7). I anticipated to rescue SHARPIN deficiency-induced skin inflammation through blocking TNF-α induced programmed cell-death in CPDM mice by creating epidermis specific TRADD KO in CPDM background. While FADD and caspase-8 genetic ablation was embryonic lethal, TRADD full body KO showed insusceptibility towards TNF-α induced apoptosis making it an ideal target gene[120-123].

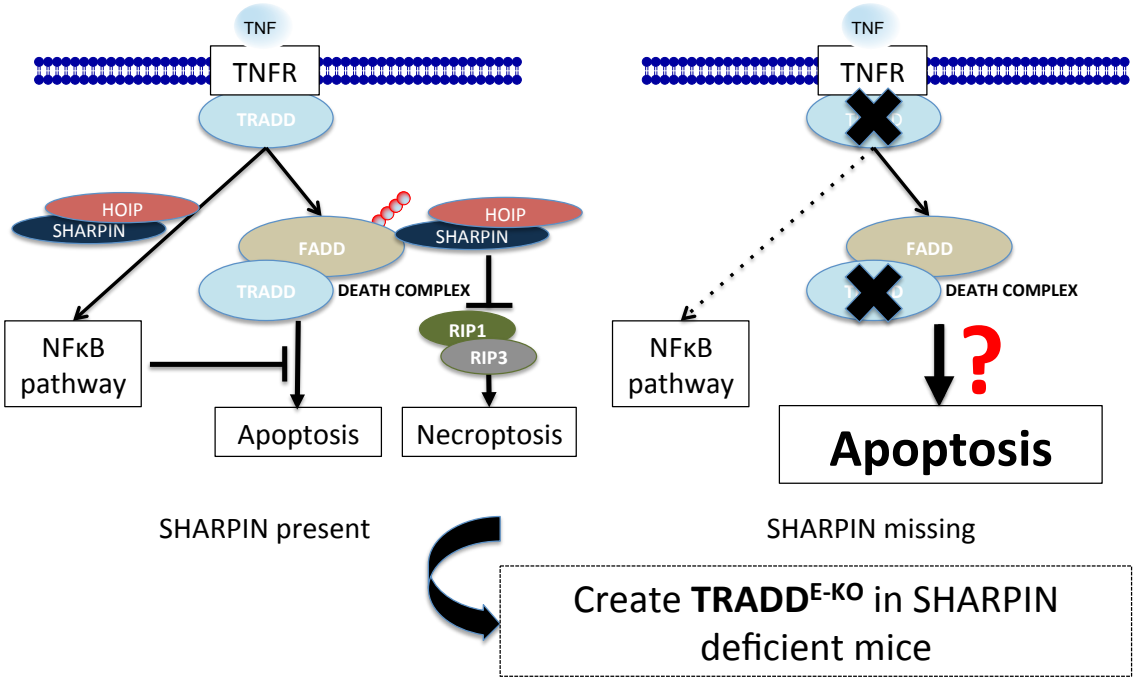

Figure 7 | TRADD skin conditional genetic ablation in CPDM mice aims to rescue skin inflammation. Depleting TRADD in skin of CPDM mice is supposed to rescue skin phenotype by blocking the death complex downstream of TNF signalling and thereby abolish proposed apoptosis induced skin inflammation. TNF: tumour necrosis factor; TRADD: TNFR1 associated protein wit death-domain; HOIP: HOIL-1L interacting protein; SHARPIN: SHANK associated RH domain-interacting protein; RIP: receptor interacting protein; FADD: Fas associated protein with death-domain

Materials and Methods

Mice

SHARPIN mutant mice were acquired from The Jackson Laboratories. $TRADD^{f/f}$ and K14-Cre mice were a kind gift from Manolis Pasparakis. Animals were kept and handled at the animal colony of the Institute of Molecular Biotechnology of the Austrian Academy of Science (IMBA) in accordance with institutional guidelines. $SHARPIN^{cp/+}$, $TRADD^{f/f}$ and $K14^{tg/+}$Cre mice were crossed and offspring genotyped for all mutations.

DNA purification

Mouse-tail tissue samples were digested and purified using Promega Wizard® Genomic DNA Purification System (Promega, A3260). Mouse-tail derived tissue samples were incubated in tail lysis buffer containing freshly added Proteinase K [2mg/mL final concentration] at 55ºC overnight. Wizard®SV Lysis buffer is added to the lysate, vortexed and transferred to spin columns and centrifuged at 13.000 x g for 3'. DNA bound to the columns is washed three times with ethanol containing Wash Solution and finally eluted with nuclease free water; 260/280nm absorption was measured to verify successful DNA purification.

Genotyping

TRADD floxed & KO allele as well as K14-cre mutant allele were identified by genotyping PCR reaction using following primers: $TRADD^{flox}$ fwd (GGCCAGACATCTCCACCGTAG), $TRADD^{flox}$ rev (TTTGCCTTCAGCCTAAGTTCC), $TRADD^{KO}$ fwd (GGCCAGACATCTCCACCGTAG), $TRADD^{KO}$ rev (GTTGTGGCGGATCTTGAAGTT), K14-cre fwd (AGCACCTTCTCTTCACTCAGC) and K14-cre rev (CGCATAACCAGTGAAACAGCAT). PCR products were loaded on 1-2% agarose gel depending on amplicon size and bands visualised under UV-light.

SHARPIN pyrosequencing

Purified DNA samples were sent for pyrosequencing (Varionostic GmbH, Ulm, Germany). DNA samples were treated with bisulphite to create single strand DNA (ssD-

NA), sequencing primer anneal to the ssDNA in the presence of adenosine-5'-phosphosulphate, luciferin, DNA polymerase, sulfurylase, luciferase and apyrase that produce a fluorescent signal upon incorporation of a single nucleotide in the elongating strand. One of the four dNTPs at a time was added to the reaction, if complementary to the ssDNA, a light signal was generated, detected by a camera and digitalised into a graph[124].

Tissue processing

Mice were sacrificed by cervical dislocation and tissues were harvested and fixed in 4% Paraformaldehyde solution overnight at RT. Fixed tissue was dehydrated overnight (Milestone LOGOS tissue processor) and embedded in paraffin for subsequent sectioning at the microtome. 2-3µm sections cut at MICROM HM 355 were dried at 55ºC for 2h to overnight for subsequent staining.

Haematoxylin and Eosin (H&E) staining

Sections were stained by haematoxylin and eosin (H&E) using Thermo Scientific Microm HMS 740 slide stainer. Coverslips were mounted on stained slides and scanned using Mirax slide scanner (Carl Zeiss).

Immunohistochemistry

Sections were deparaffinised, endogenous peroxidase activity was blocked with 1x peroxidase blocking buffer [0.04M Na-Citrate, 0.121M Na_2HPO_4, 0.03M NaN_3, 3%H2O] and antigen retrieval was achieved by proteinase K (Sigma, #P2308) digestion in TEX buffer [50mM Tris-HCl pH8, 1mM EDTA, 0.5% Triton-X] or by boiling at 95°*C* in retrieval buffer [10mM Na-Citrate buffer pH6, fresh 0.05% Tween-20) depending on primary antibody. Unspecific binding was blocked by incubation with blocking buffer [10% Normal goat serum, 0.3% Triton-X + 16% Avidin D (VectorLab Avidin/Biotin blocking kit, #SP-2001)]. The following primary antibodies were used: K14, K6 from Covance (Princeton, USA); F4/80 (clone A3-1) from AbD Serotec; cleaved caspase-3 (#9664) from Cell Signaling; TRADD (H-278) from Santa Cruz. Antibodies were incubated in blocking solution containing 16% Biotin (VectorLab Avidin/Biotin blocking kit,

#SP-2001) overnight. Secondary antibodies coupled to Biotin (Dako) were incubated in blocking solution; signal was amplified by avidin-biotin-HRP detection system (ABC VectorLab Elite Kit, #PK-6100) and detected by peroxidase substrate (VectorLab NovaRed, #SK-4800). Sections were counterstained with hematoxylin for nuclei visualization.

Immunofluorescence

Cells were fixed in 4% paraformaldehyde, permeabilised in 0,1%Triton/PBS, blocked in NGS/BSA/0,05% Triton in PBS and incubated with anti-cleaved caspase-3 (Cell Signaling; #9664) followed by incubation with Alexa488 coupled anti-rabbit antibody (Invitrogen, #A11008). Nuclei were stained by DAPI.

Immunoblotting

Samples were boiled in SDS sample buffer [0.125M Tris-HCl, 0.1% SDS w/v ph6.8; 20% Glycerol, 2% SDS, bromphenolblue, 5% beta-mercaptoethanol] and separated by SDS-PAGE gel electrophoresis. 4-12% gradient gels (Bio-Rad, #456-1091) were run in SDS running buffer [25mM Tris, 0.2M Glycine, 0.1% SDS] and transferred on nitrocellulose membrane (Bio-Rad, #170-4270) using semidry transfer system (Bio-Rad TransBlot®Turbo™, #170-4155). Membrane was blocked in TBS with 5% BSA, 0.1%NaN_3 and incubated with primary antibodies o/n at 4°*C*. Following antibodies were used: Ub P4D1 (#3936), cleaved caspase 3 (#9664), PARP (#9542) from Cell Signalling and vinculin (#V9131) from Sigma-Aldrich. Secondary HRP-labelled antibodies were used, developed by ECL (Santa Cruz, #sc-2048) and signal detected with light sensitive films.

Cell culture

Mouse embryonic fibroblasts were maintained in Dulbecco's Modified Eagle's Medium (DMEM) with 10% fetal calf serum and 1% penicillin/streptomycin. Cells were kept under standard conditions (37°*C*, 5% CO_2) and split every 2-3 days with 1x trypsin 0.25% EDTA (Invitrogen, #25200-056).

Primary keratinocytes were isolated from adult mouse-tail skin. Mice were sacrificed, tail was cut and immersed with 70% ethanol and put in ice-cold PBS. A longitudi-

nal incision was made; the skin was peeled off and digested in KFSM media (Invitrogen, #17005-042) with 2U/mL dispase II (Invitrogen, #17105-041) at 4°*C* overnight. Epidermis was separated from dermis, incubated in trypsin LE express (Invitrogen, #12605-010) at 37°*C*. After centrifugation, cell pellet was resuspended and seeded in collagen IV (Sigma, #C7521) coated plates and kept under standard conditions. The next day media was changed prior cytokine stimulation.

Apoptosis assessment

MEF cells (0,05 x 10^6) were seeded per 24-well. Cells were washed and media changed before addition of TNF-α (PeproTech, #315-01A) and cycloheximide (Sigma, #C7698) at the indicated concentrations and time period. The percentage of apoptotic cells was quantified by fluorophore coupled Annexin V antibody (BD Bioscience, #556419) staining and PI uptake. Samples were analysed by flow cytometry (FACS Canto, BD Bioscience). Additionally, total cell lysates were prepared and apoptosis induction evaluated by immunoblotting against cleaved caspase 3 (#9664) and PARP (#9542) from Cell Signalling.

Recombinant protein purification

HOIP, HOIL and SHARPIN pGex-Gp1 containing expression plasmids were transformed into BL21 (DE3) E.Coli (IMBA Molecular Biology Service), single colony overnight cultures were used to inoculate 1L pre-warmed LB-Amp media and grown till OD~0.5. Bacteria were induced with IPTG at 16°*C* overnight. Cells were harvested by centrifugation, pellet resuspended in lysis buffer [PBS pH7.3, 1mM PMSF, 1mM DTT] and lysed by sonication. Subsequently, lysate was centrifuged and supernatant sterile filtered prior application on GSTrap HP column (GE Healthcare, #17-5281-01) employing Äkta explorer FPLC (GE Healthcare, ÄKTAexplorer 10). Filtered supernatant was loaded slowly onto equilibrated column; column was washed with excess of binding buffer [PBS pH7.3, 1mM DTT] and afterwards equilibrated with cleavage buffer [50mM Tris-HCl, 150mM NaCl, 1mM EDTA, 1mM DTT pH7.5]. Subsequently, precision protease is applied on the column and incubated under rotation overnight at 4°*C*. The next day, cleaved-off

protein is collected using Äkta fraction collector (GE Healthcare, Frac-950). A280nm peak fractions were loaded on SDS-PAGE and stained by coomassie brilliant blue [0.25% Coomassie blue, 45% Methanol, 10% Acetic acid].

In Vitro Ubiquitination assay

Ub (7.5µg), E1 (150ng), UbcH7 (150ng) from Boston Biochem together with recombinant purified E3 ligase complex were incubated with and without ATP (Sigma) in assay buffer [20mM Tris-HCl ph7.5, 5mM $MgCl_2$, 2mM DTT, 1.5% Glycerol] at 37°*C* overnight. Reaction was stopped by addition of SDS sample buffer; samples were boiled at 95°*C* for 1min and subsequently Ub chain formation was detected by anti Ub P4D1 specific immunoblotting.

Immune cell profiling

Tissues were harvested from age matching mice incubated with Collagenese 4 (100µg/mL), Liberase TM (100µg/mL) and DNase (50µg/mL) in IMDM at 37°*C* for 2hrs. Resuspend tissue and smash through 70µm cell-strainer and perform antibody staining. Following antibodies were used: TCR-β (H57-597), TCRγδ (GL3), CD4 (PM4-5), CD8a (53-6.7), Nk1.1 (PK136), CD45 (30-F11), Ly6G (Ia8), B220 (RA3-6B2), CD11b (m1/70), CD11c (HL3) from Biolegend; FoxP3 and e780 viability dye from eBioscience. Cells were plated in 96-well, washed with FACS buffer (2% FCS in PBS), dead cells excluded by e780 viability dye staining and Fc blocking was performed. Surface markers were stained; afterwards, cells were fixed and permeabilised with FoxP3 permeabilisation/fixation kit (eBioscience, #00-5521-00) and intracellularly stained for FoxP3. Samples were analysed by flow cytometry (FACS Fortessa LSR, BD Bioscience).

Results

Recombinant LUBAC generates free linear-Ub chains

LUBAC components HOIP, HOIL-1L and SHARPIN were purified from an E.Coli expression system. Large (120kDa) HOIP protein is weakly expressed and unstable, whereas smaller LUBAC components HOIL-1L (50kDa) and SHARPIN (40kDa) are more stable but still show degradation bands (Figure 8B).

Ub E3 ligase activity was assessed by *in vitro* ubiquitination assay. Assembling LUBAC comprised of all three subunits together and performing an *in vitro* ubiquitination experiment, showed potent Ub chain formation (Figure 8A).

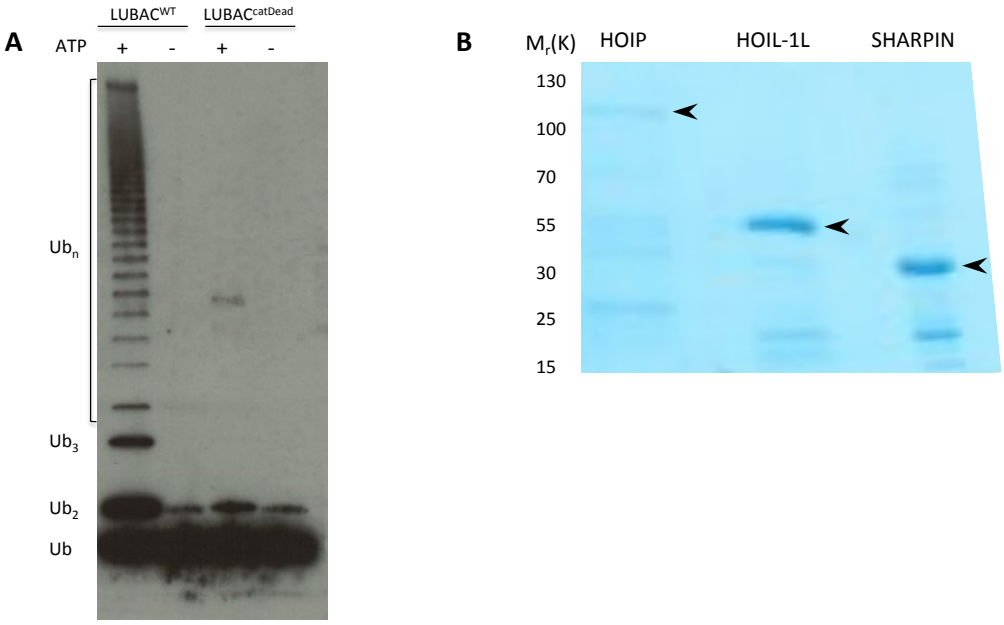

Figure 8 | Recombinant purified LUBAC generates free Ub chains. A Free Ub chain formation by LUBAC^{WT} in in vitro ubiquitination assay and assessed through immunoblotting using anti-Ub specific antibody. A LUBAC^{catDead} complex comprised of a HOIP Ring1Ring2 mutant is incapable of Ub chain formation. **B** Coomassie staining of purified LUBAC components indicated by arrows. Ub, Ubiquitin; LUBAC, Linear Ub Chain Assembly Complex; HOIP: HOIL-1L interacting protein; HOIL-1L: Heme-oxidised iron-regulatory protein 2 Ub ligase 1L; SHARPIN: SHANK associated RH domain-interacting protein

The antibody used for immunblotting recognises Ub itself but does discriminate amongst the various chain types. LUBAC generated Ub chains were exclusively N-

terminally linked through Met1. Additional experiments with lysine less Ub mutants and methylated Ub moieties showed unaffected or failing free-Ub chain formation respectively[20]. Furthermore, samples were analysed by mass spectrometry confirming primarily linkage between N-terminal Met1 and C-terminal glycine[20]. Hence, my recombinant LUBAC generates lin-Ub chains *in vitro* (Figure 8A).

Catalytic dead HOIP Ring1Ring2 (C699, 702, 871, 874S) was purified and utilised to conduct *in vitro* ubiquitination with HOIL-1L and SHARPIN in complex. HOIP C-terminal RBR region is essential for its catalytic activity. Mutations in crucial cysteines for zinc-finger coordination and thioester-formation in the Ring1 and 2 are unable of Ub-chain formation (Figure 8A).

Albeit, recombinant LUBAC potently generates free Ub chains *in vitro*, previously shown substrate ubiquitination of cell-death component FADD (unpublished) could not be observed possibly due to technical problems (data not shown).

SHARPIN deficiency causes a severe overt phenotype

Skin of WT and CPDM mice was subjected to H&E staining and immunohistochemistry antibody staining for macrophages and apoptotic cells. CPDM mice showed apparent cpdm skin phenotype and were moderately smaller than littermates (Figure 9). Histological analyses revealed previously described hyperkeratosis, hyperplasia and parakeratosis as well as macrophage infiltration and apoptotic cells that could not be observed in WT skin (Figure 9). Hence, CPDM mice suffer from severe skin inflammation characterised by innate immune cell infiltrates and apoptotic keratinocytes.

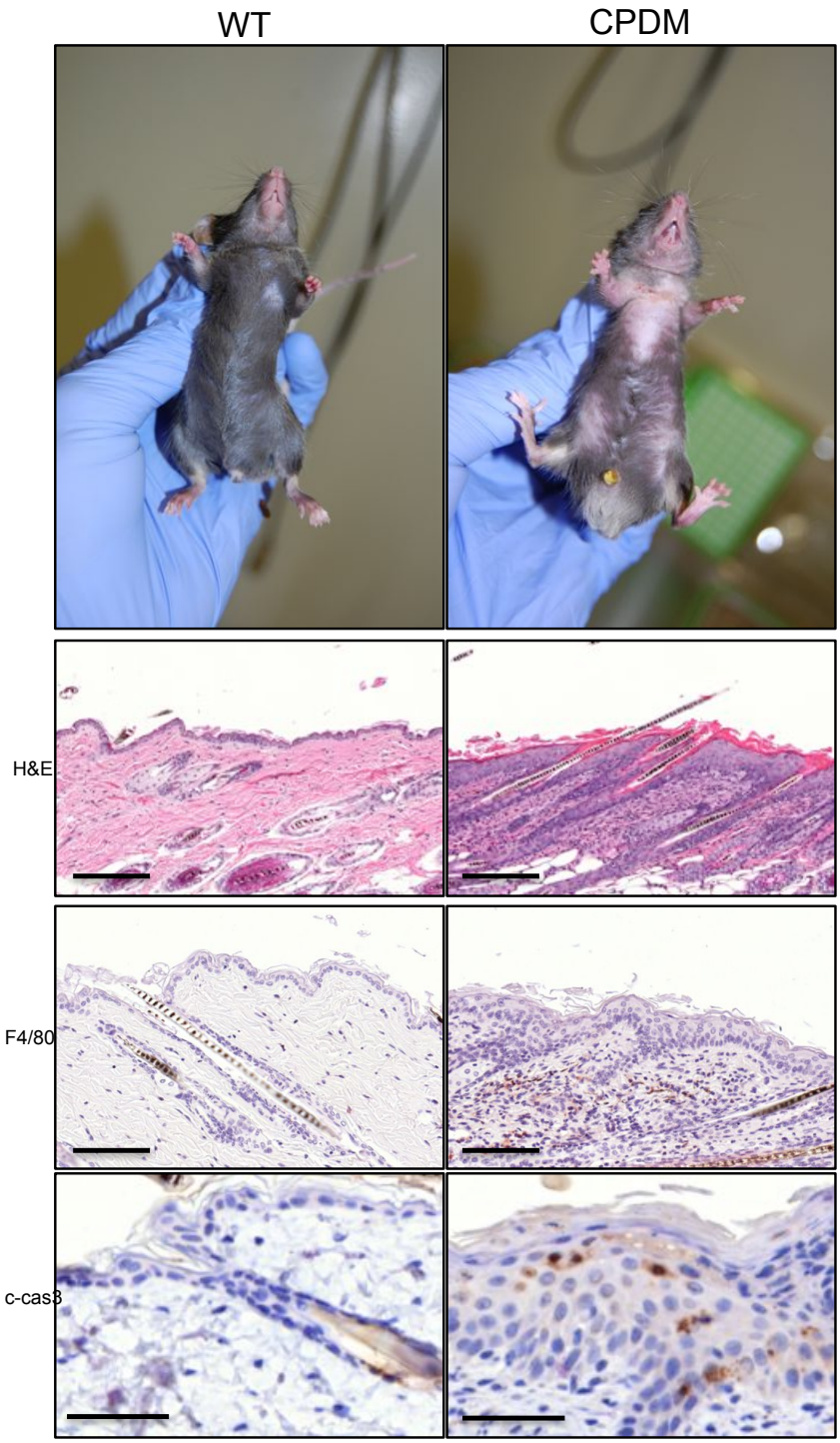

Figure 9 | CPDM mice show severe skin lesions, macrophage infiltration and apoptotic keratinocytes. Top lane, gross appearance of WT and CPDM mice; CPDM mice suffer from skin inflammation starting at 3 weeks of age. H&E staining showed skin lesions and macrophage infiltration (F4/80) not seen in WT skin tissue. C-cas3 staining shows apoptotic keratinocytes. Scale bar lane 2,3 100µm and lane 4 50µm. C-cas: cleaved caspase-3

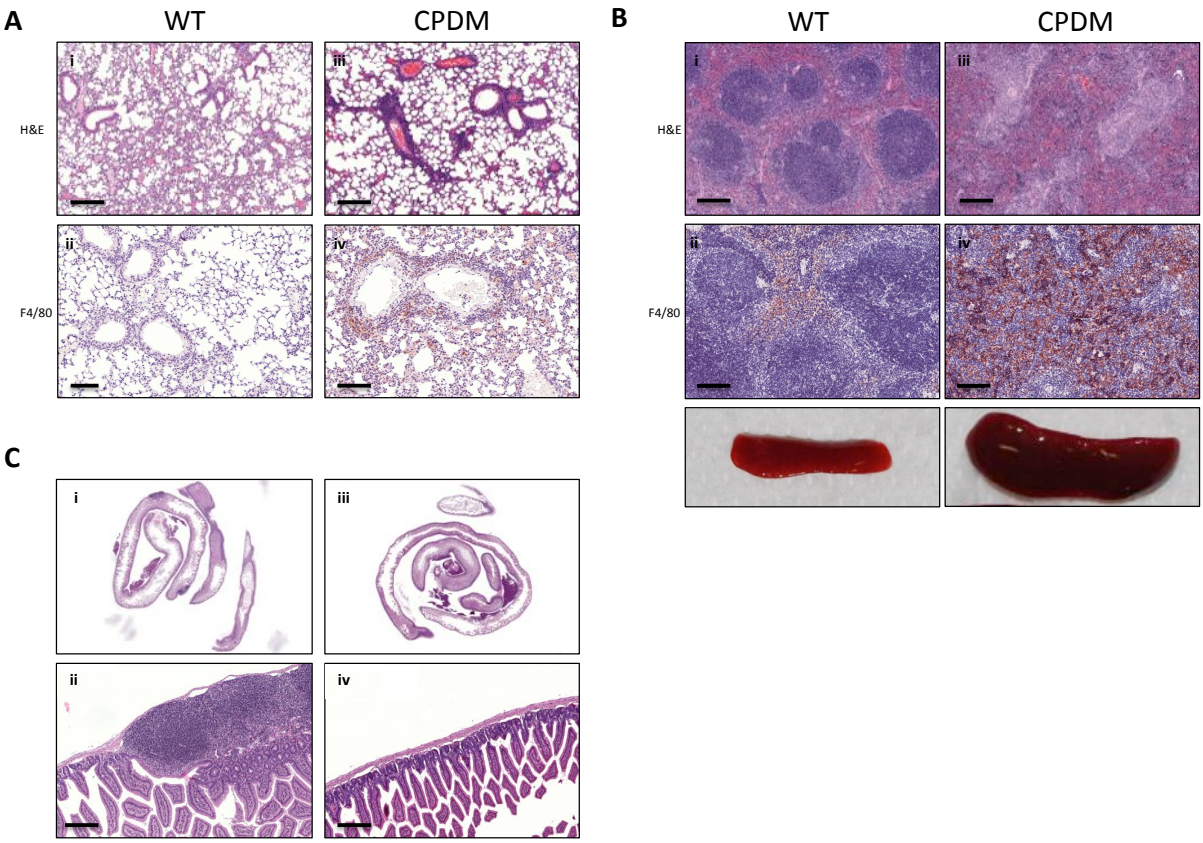

Figure 10 | CPDM mice present multi-organ phenotype. A CPDM lung blood vessel epithelial cells are thickened and infiltrated by macrophages as seen by H&E (iii) and F4/80 (iv) staining respectively. **B** CPDM mouse spleen is enlarged (bottom) compared to WT littermate control. Germinal centre formation is defective (iii) spleen is infiltrated by macrophages shown by F4/80 staining (iv) in spleen of CPDM mice. **C** Organised peyer's patches are absent in CPDM small intestines (iii & iv). Scale bar 200µm A(i,iii), B(i,iii) and C(ii,iv); 100µm A(ii,iv) and B(ii,iv).

Lung, spleen and small intestines were harvested from age matching WT and CPDM mice and histologically analysed. Blood vessels in CPDM mice derived lung tissue were enlarged and were infiltrated by macrophages (Figure 10A). CPDM spleen was characterised by splenomegaly, defective germinal centre formation and macrophage infiltration (Figure 10B). Organised peyer's patches were not found in the small intestines of adult CPDM mice (Figure 10C). Thus, CPDM mice showed previously described[55-57,119] defects of the cpdm phenotype.

SHARPIN deficiency enhances apoptosis in MEF upon TNF-α stimulation

Besides Nf-κB activation, TNF signalling also induces FADD-caspase-8 mediated apoptosis through DISC. Apoptosis induction was assessed after TNF-α and cycloheximide (CHX) stimulation in WT and CPDM derived MEF.

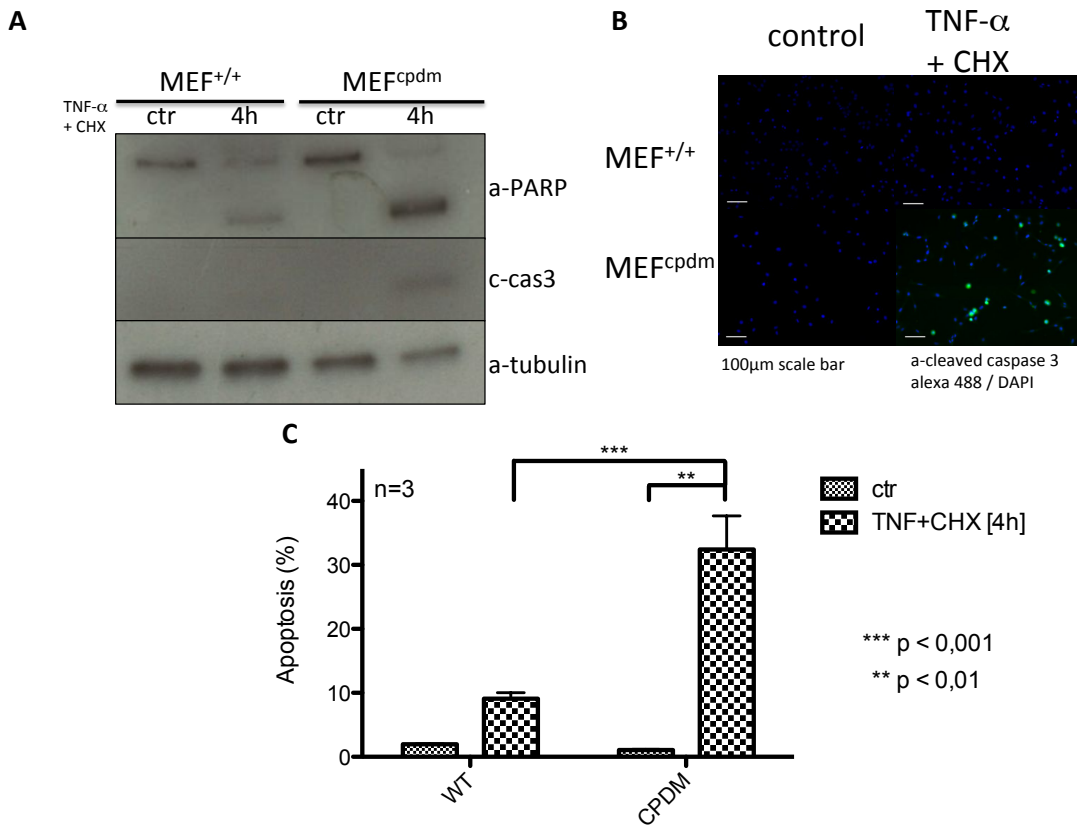

Figure 11 | Loss of SHARPIN sensitises MEF to TNF mediated programmed cell-death. A Immunoblotting for cell-death markers PARP and cleaved caspase 3. **B** IF staining of cleaved caspase 3 after cytokine stimulation and DAPI counterstaining. **C** Quantification of apoptosis in WT and CPDM MEF. C-cas3: cleaved caspase-3; TNF: tumour necrosis factor alpha; PARP: Poly (ADP-ribose) polymerase; CHX: cycloheximide

CPDM MEF were hypersensitive for TNF-α induced apoptosis determined by increased effector caspase-3 and its substrate PARP (Poly (ADP-ribose) polymerase) proteolytic cleavage using specific antibodies for immunoblotting (Figure 11A). According-

ly, cleaved caspase-3 specific IF staining shows apoptotic cells (green) in CPDM MEF after cytokine treatment but not in WT or untreated control MEF (Figure 11B). AnnexinV/PI stain and subsequent flow cytometry based quantification revealed that CPDM MEF are significantly ($p<0,001$) more sensitive to TNF-α/CHX stimulation than WT MEF (Figure 11C).

CPDM mice show up-regulation of apoptosis in keratinocytes

Primary keratinocytes of CPDM and WT mice were isolated for short time culture, cytokine stimulation and flow cytometry based apoptosis quantification.

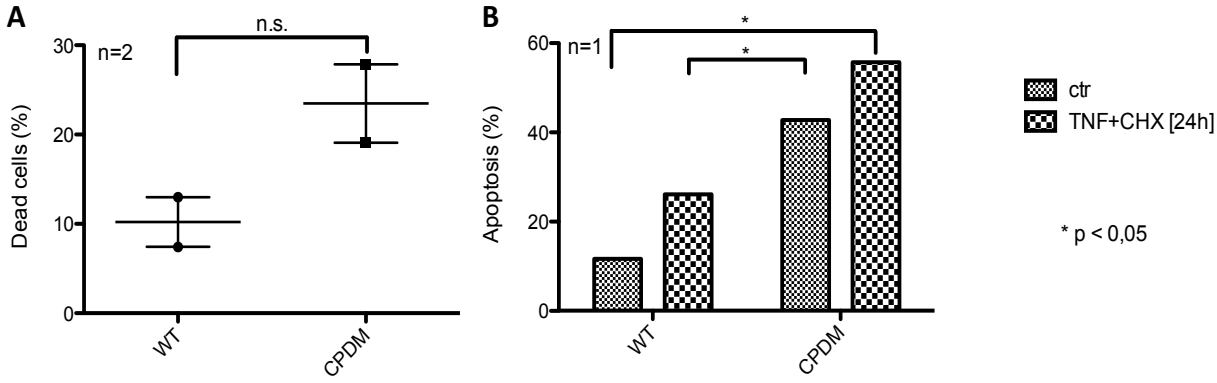

Figure 12 | Apoptosis in CPDM derived primary keratinocytes is up-regulated. A Tail-derived primary keratinocytes of 2 mice were analysed for percentage of dead cells. **B** Primary keratinocytes of 3 mice per genotype were pooled, stimulated and apoptosis assessed. TNF: tumour necrosis factor alpha; CHX: cycloheximide; n.s.: not significant

Apoptotic cells were found by cleaved caspase-3 immunohistochemical staining in the skin of CPDM mice (Figure 9) and in CPDM mice derived MEF (Figure 11) and hence I wanted to look at general cell-death levels and percentage of apoptotic cells after TNF-α/CHX induction in primary cell culture. Primary mouse-tail derived keratinocytes (n=2) of WT and CPDM mice were harvested and cell-death was measured by PI uptake. The preliminary data showed that CPDM primary keratinocytes had elevated levels of cell death compared to WT (Figure 12A). Primary keratinocytes of three CPDM and WT mice were pooled and apoptosis quantified after TNF-α/CHX stimulation for 24 hours. Apoptosis induction was significantly elevated in CPDM derived keratinocytes ($p < 0,05$)

upon cytokine stimulation but also highly increased in untreated CPDM control compared to WT apoptosis percentage (Figure 12B). My preliminary data suggests that keratinocytes isolated from CPDM mice have endogenously elevated levels of cell-death and are more susceptible towards cytokine-induced apoptosis.

CPDM mice featured aberrant numbers of regulatory T-cells

The cpdm phenotype is characterised by severe skin inflammation and defects in organs of the immune system (Figure 9 & Figure 10). Therefore, spleen, draining lymph node and skin tissue were analysed for their immune cell profiles to reveal possible implications of the immune system in the phenotypes. Cells were isolated, subjected to surface as well as intracellular staining and subsequently analysed by FACS.

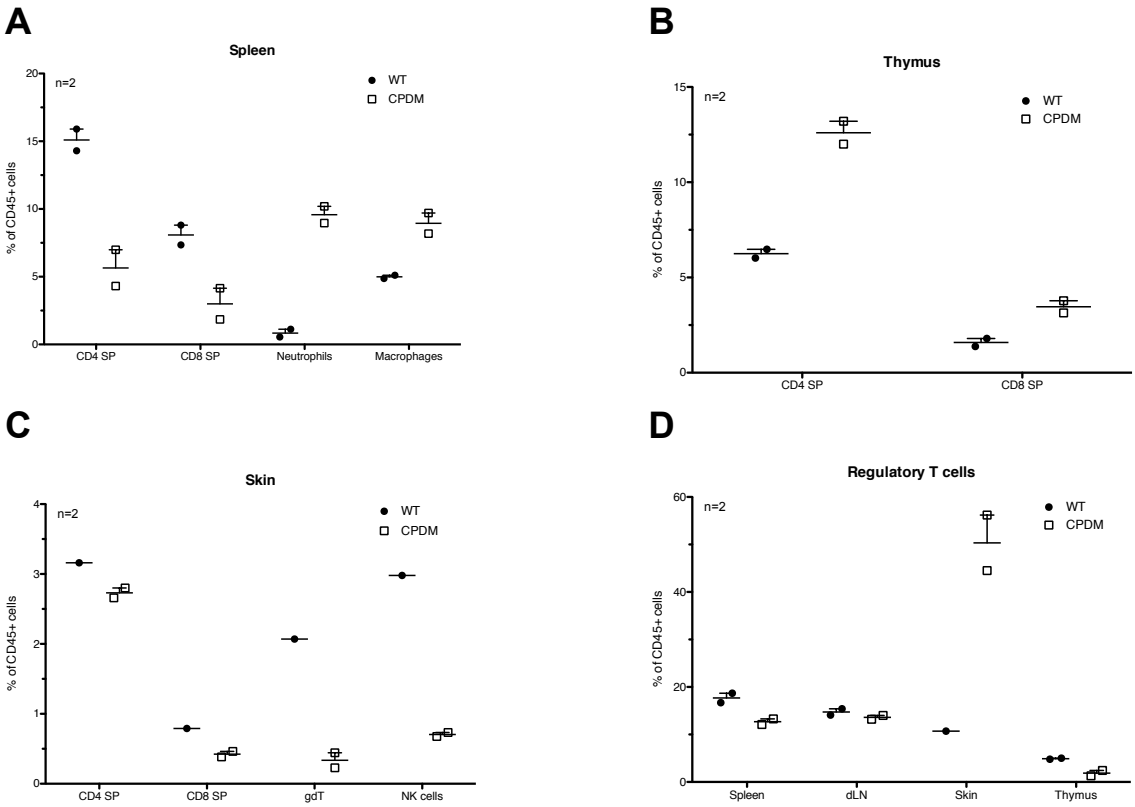

Figure 13 | Immune cell profile of WT and CPDM mice. A CPDM derived spleen showed deprivation of CD4 and CD8 single positive T-cells and up-regulation of innate immune cells (neutrophils & macrophages). **B** CD4 and CD8 levels are elevated in the thymus of CPDM mice. **C** The skin of CPDM mice had reduced numbers of T-cells (CD4, CD8 &

gamma delta T-cells) as wells as natural killer cells. **D** CPDM skin presented 4 times increase in regulatory T-cell number whilst other tissues showed a slight decrease in regulatory T-cell number.

Consistent with immunohistochemistry staining of CPDM spleen tissue (Figure 10B), numbers of macrophages are elevated; additionally, neutrophils infiltrate the spleen. Furthermore, spleen is depleted of immune cells represented by lower numbers of T-cells (Figure 13A). In response to the multi-system disease, thymus of CPDM mice was enlarged and had increased repertoire of T-cells (Figure 13B). Cells isolated from skin tissue had an overall raise in CD45 positive cells (Figure 14), whereas single positive T-cells and natural killer cell numbers are lower compared to WT skin tissue (Figure 13 & Figure 14). Noteworthy, cells positive for the transcription factor FoxP3, master regulator of regulatory T-cell (Tregs) development and function, were highly increased in CPDM mice skin tissue (Figure 13D). Interestingly, in spleen, draining lymph nodes and thymus the numbers were slightly below WT levels suggesting a possible defect in central Treg mediated tolerance (Figure 13D).

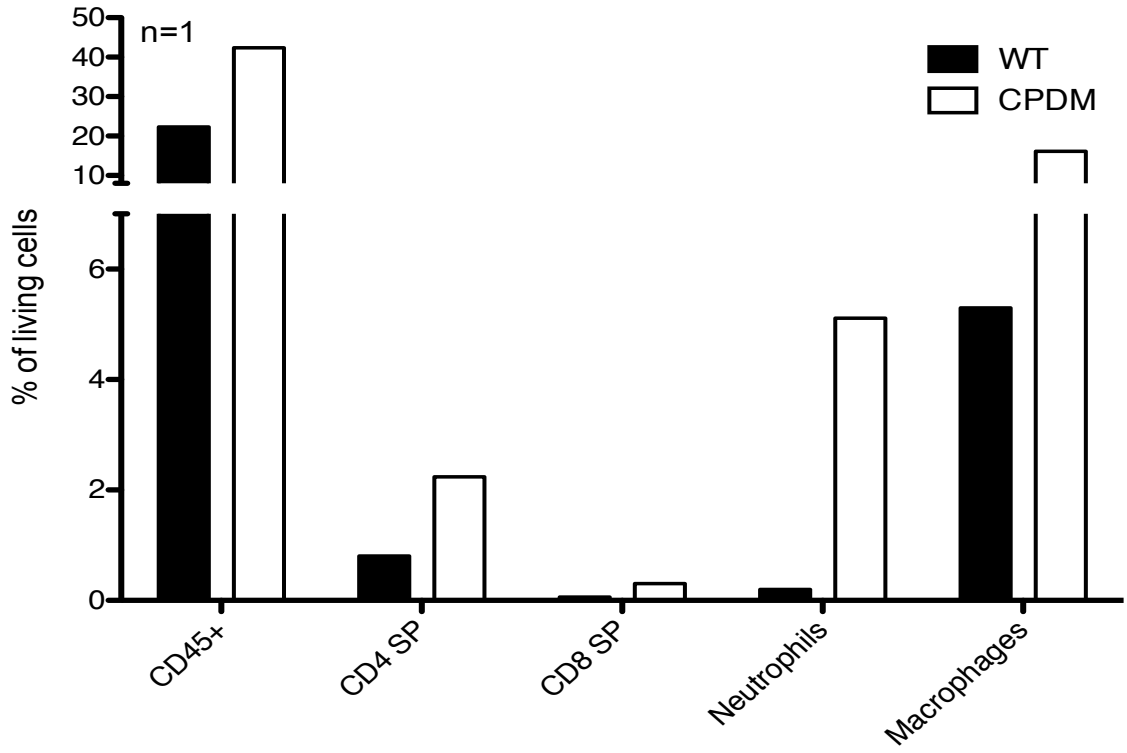

Figure 14 | Innate immune cells are increased in skin of CPDM mice. Overall increase of CD45 positive cells could be observed. Furthermore, innate immune cells were highly increased.

Skin tissue of CPDM mice was characterised by highly elevated number of CD45 cells and showed a strong innate immune response presented by enlarged number of macrophages and neutrophils (Figure 14). My preliminary data analysing a small number supports previous reports that innate immune cells predominantly drive skin inflammation and the adaptive responses are subordinate and give a possible twist for a role of Tregs in cpdm phenotype.

Skin inflammation was rescued in CPDM.TRADD$^{E\text{-}KO}$ mice

We anticipated to rescue cpdm skin phenotype by introducing an epidermis conditional TRADD knockout (TRADD$^{E\text{-}KO}$) in CPDM mice background to block TNF signalling induced apoptosis[122,123,125].

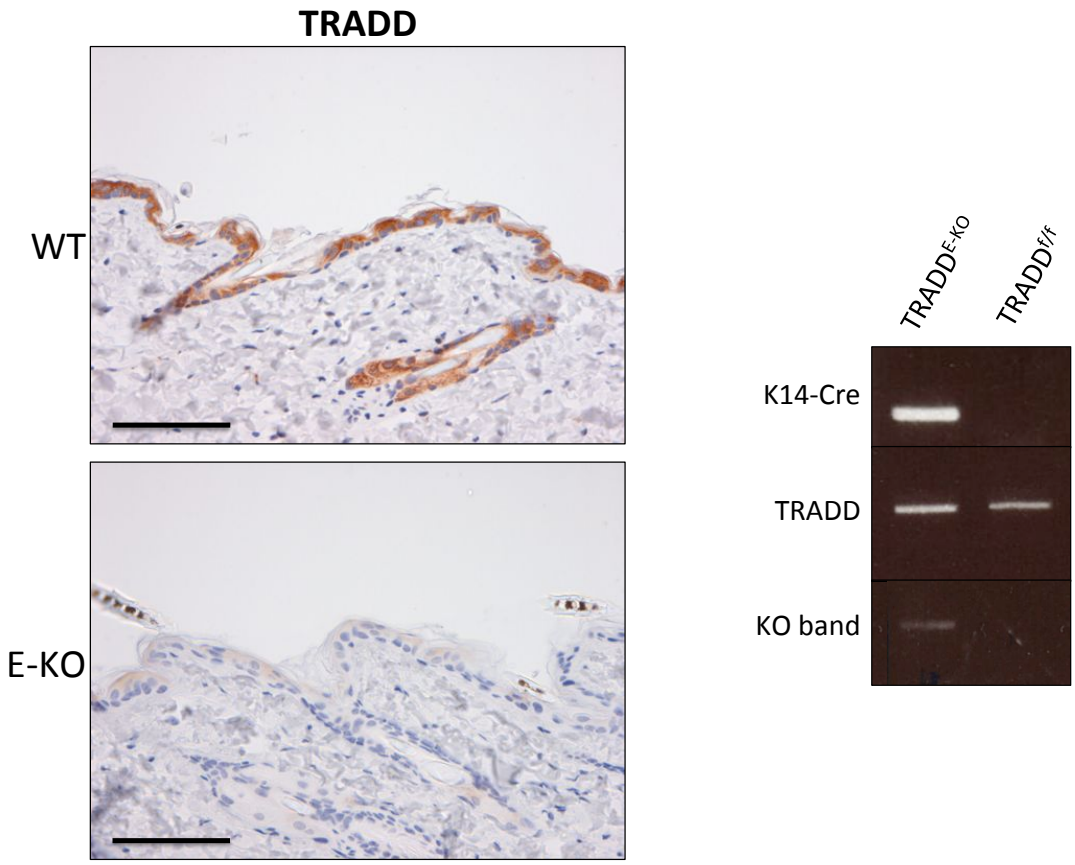

Figure 15 | TRADD$^{E\text{-}KO}$ skin tissue is genetically ablated for TRADD. Immunohistochemistry staining of TRADD$^{f/f}$ and TRADD$^{E\text{-}KO}$ skin sections showed complete TRADD deficiency. 100µm scale bar

Mice carrying floxed TRADD alleles were crossed with a keratin-14 (K14) epidermis specific cre-recombinase expressing mice; PCR genotyping and TRADD specific immunohistochemistry staining confirmed the skin conditional knockout (Figure 15).

I obtained the desired genotype after several generations of crosses of SHARPIN$^{cpdm/+}$ with TRADD$^{E\text{-}KO}$ mice. Skin tissue was harvested of age matching mice (n=1, 9w old) and subjected to immunohistochemical staining for K14, cleaved caspase-3, F4/80 and TRADD as well as standard H&E. WT skin presented completely normal skin architecture (Figure 16 1st lane). In contrast, CPDM skin presented overt inflammatory phenotype including epidermal hyperkeratosis, hyperplasia and parakeratosis as well as described apoptotic nuclei and macrophage infiltration (Figure 16 2nd lane). All heterozygous control showed no apparent phenotype and resembled WT skin (Figure 16 3rd

lane). Strikingly, CPDM.TRADD$^{E\text{-}KO}$ skin showed a complete rescue and WT appearance (Figure 16 4th lane). Different tissue samples – both dorsal and ventral – showed similar rescue of the cpdm phenotype. My findings indicate that TRADD epidermis specific depletion is sufficient to reverse SHARPIN deficiency induced skin disease and further favours the hypothesised cross-talk between TNF-α induced apoptosis and inflammation.

TRADD$^{E\text{-}KO}$ does not or only partially alters cpdm multi-organ phenotype

Besides skin inflammation, CPDM mice suffer from a multi-organ phenotype including defects in spleen, lung and liver and absence of peyer's patches[54,57]. Age matching mice (n=1, 9w old) were sacrificed and respected tissues were harvested for sectioning and H&E staining (Figure 17). WT tissue sections and spleen gross appearance looked completely normal (Figure 17 1st lane), whereas in CPDM samples characteristic SHARPIN deficiency induced infiltrates, defective spleen germinal centre formation and size increase as well the absence of peyer's patches could be observed **(**Figure 17 2nd lane).

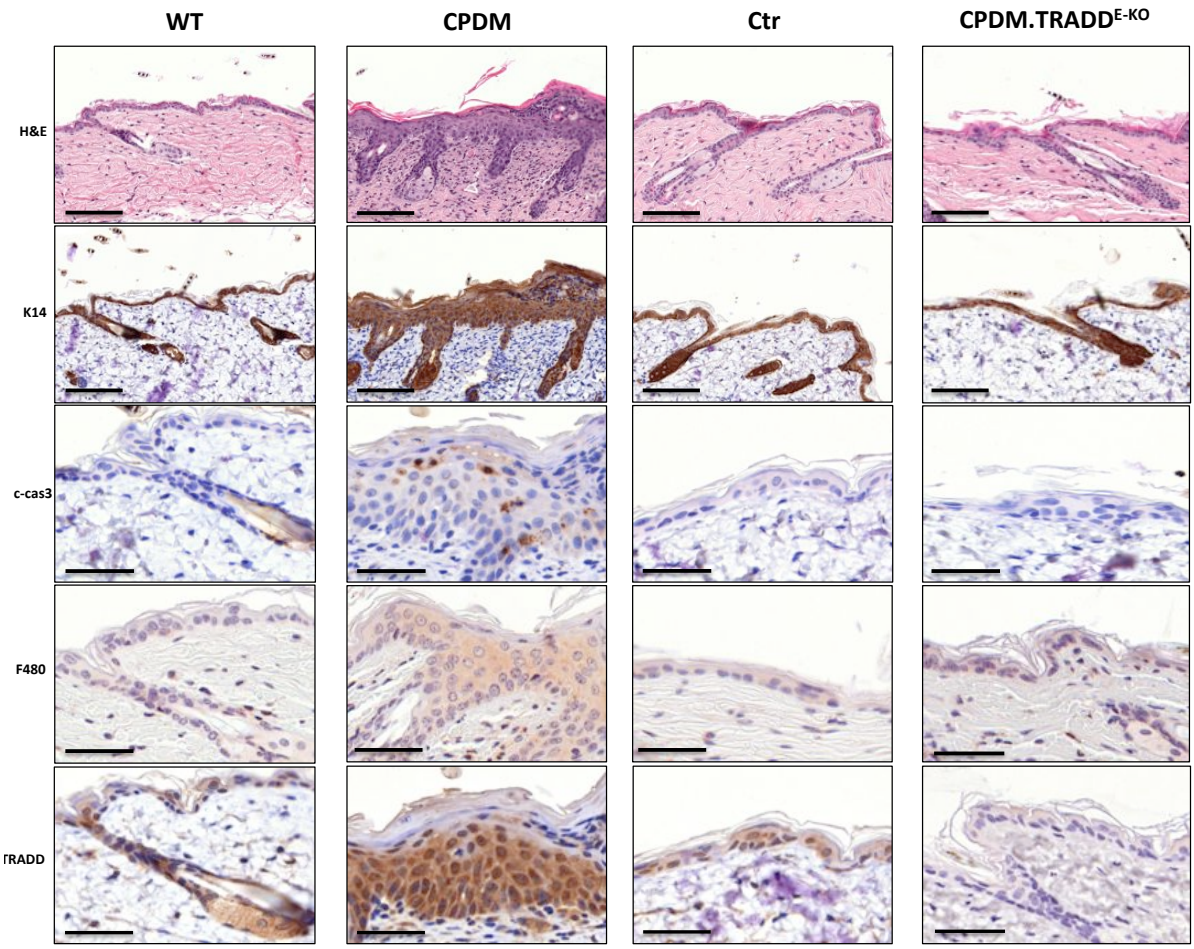

Figure 16 | CPDM skin phenotype was rescued after crossing SHARPIN deficient mice with TRADD^{E-KO} mice. CPDM skin tissue (2nd lane) characterised by epidermal thickening (H&E & K14), cleaved caspase-3 positive cells and macrophage infiltration (F4/80) was rescued in SHARPIN$^{cp/cp}$.TRADD^{E-KO} mice (4th lane). Scale bar 100µm row 1 &2 and 50µm row 3,4 & 5.

All heterozygous control (Figure 17 3rd lane) showed no apparent effects. Noteworthy, CPDM.TRADD^{E-KO} mice revealed to be mostly unaffected regarding cpdm multi-organ phenotype as peyer's patches were absent and lung showed immune cell infiltrates (Figure 17 4th lane). Though, defects in liver, and especially in spleen seemed to be milder compared to severely defective spleen organisation and size enlargement in CPDM mice (Figure 17 2nd lane).

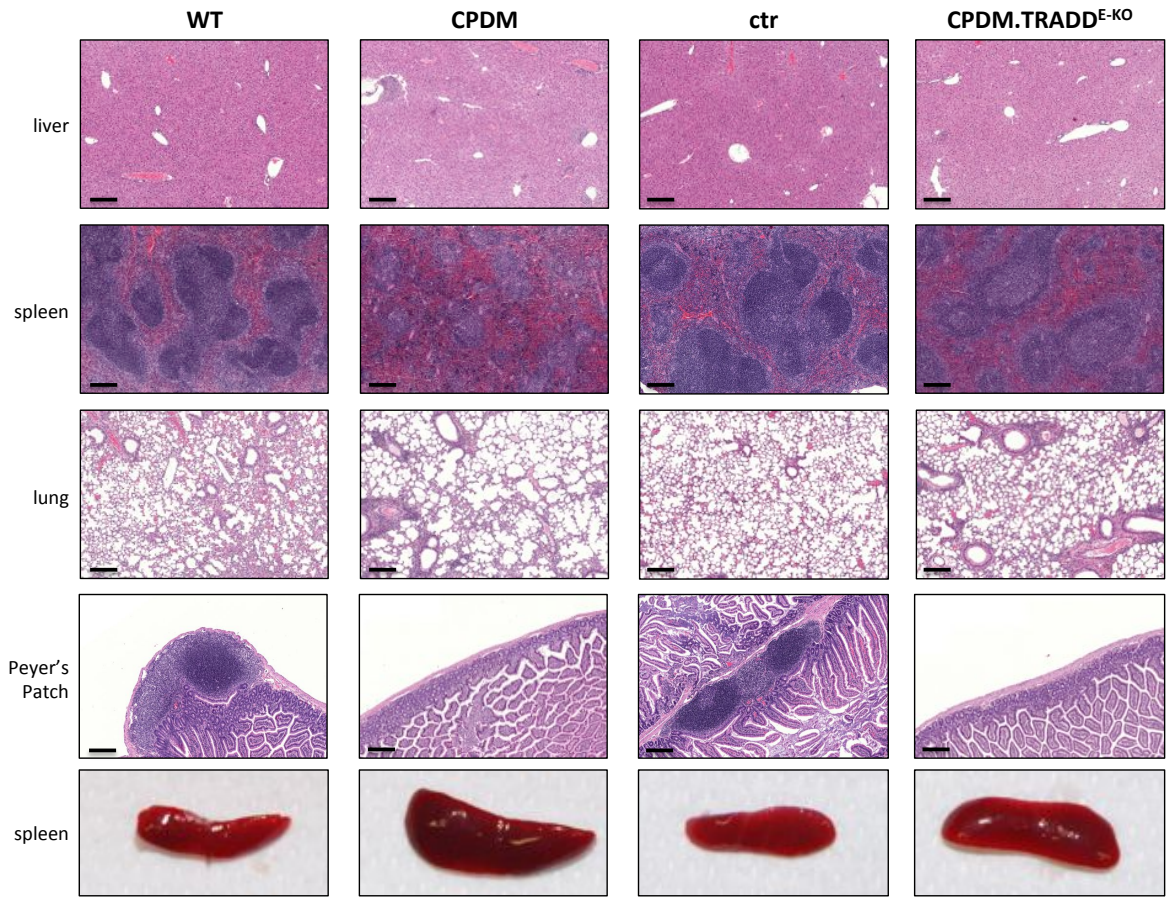

Figure 17 | cpdm phenotype is not affected in CPDM.TRADD^{E-KO} mice. WT tissues (1st lane), normal liver, lung and spleen architecture as well as visible peyer's patch formation in small intestine. Tissue sections from CPDM mice (2nd lane) presented typical innate immune cell infiltrates in liver and lung, defective spleen germinal centre formation and increase in size as well as absent peyer's patch formation. SHARPIN deficiency induced multi-organ defects were not rescued in CPDM.TRADD^{E-KO} animals (4th lane). Scale bar 200µm.

Summarised, CPDM.TRADD^{E-KO} mice developed cpdm phenotype endorsed by e.g. lack of peyer's patches; yet, less pronounced defects in lung and spleen indicated a potential partial rescue mechanism of cpdm phenotypes in respected organs but needs further investigation.

Discussion

Recombinant LUBAC generates linear Ub chains *in vitro*

SHARPIN controls apoptosis upon TNF-α binding to the TNFR1, presumably destabilising the later forming death induced signalling complex (DISC) through specifically interacting and linearly ubiquitinating the complex member FADD as shown by GST-pull down and *in vitro* ubiquitination assay respectively (not published). Anti-apoptotic protein ABIN1 is assumed to be recruited to modified FADD via its UBAN domain and inhibits caspase-8 – FADD binding and hence blocks caspase cascade[126]. In vitro ubiquitination assays demonstrated the high Ub ligase activity of E.Coli purified mulitsubunit E3 ligase LUBAC (Figure 8A). Binding sites that mediate FADD binding to SHARPIN in the LUBAC complex are unidentified. Possibly, conditions in the *in vitro* reaction did not favour stable interaction and hence rendered substrate ubiquitination impossible. Further studies are needed to assess how FADD gets recruited and binds to LUBAC via SHARPIN; additionally, mechanism and structure data on LUBAC mediated substrate ubiquitination are still missing.

CPDM mice display apparent cpdm phenotype

Mice carrying the single point deletion in the SHARPIN gene[54] were histologically analysed and compared to WT littermates. Skin of CPDM mice was characterised by inflammatory skin lesions with macrophage infiltration, hyperkeratosis, hyperplasia, parakeratosis and apoptotic keratinocytes (Figure 9). Internal organs were affected and resembled previously reported defects (Figure 10)[55-57,119]. In accordance with previous data, my results indicate a SHARPIN specific role in development of peyer's patches and for proper spleen formation[57,119]. Intriguingly mice lacking e.g. RelB or TNF also showed defects in organogenesis of lymph nodes, whereas in CPDM mice they develop normally[127,128]. Heterozygous TNF KO in CPDM background rescued skin phenotype bud did not affect lack of peyer's or defects in spleen[42]; hence, cpdm immune-system defects may arise independent of TNF signalling. Additionally, bone marrow transplants in irradiated

CPDM mice did not prevent loss of peyer's patches in adult mice, further providing evidence that cpdm phenotypes are not driven by the hematopoietic system[57].

SHARPIN deficiency leads to hyper up-regulation of apoptosis

TNF-α induced apoptosis induction was assessed and quantified in CPDM MEF cell line (Figure 11); furthermore, number of apoptotic cells in primary keratinocytes was measured (Figure 12). In both experiments, apoptosis was up-regulated upon cytokine treatment if SHARPIN was missing compared to WT cells. Primary keratinocytes of CPDM mice showed elevated levels of cell-death (Figure 12A) when kept in culture and hence strongly biased apoptosis quantification after TNF-α/CHX stimulation (Figure 12B). My data strongly underlines the very specific role of SHARPIN in TNF-α induced apoptosis signalling. Further experiments, increasing sample size and optimised cell culture conditions are needed to verify elevated cell-death levels in CPDM skin and higher sensitivity to apoptosis after cytokine treatment.

Immune cell composition in CPDM mice are aberrant

Pathologies in SHARPIN deficient mice, focusing in lymphoid organs, have been intensively studied over the past years[129]. In pilot experiments, skin tissue of CPDM and WT mice were examined regarding their immune cell populations. I provided further evidence to histology data, that innate immune cells drive skin inflammation (Figure 13C and Figure 14). Intriguingly, number of regulator T-cells (Tregs) were 3- to 4-fold increased in CPDM skin tissue whilst being decreased in spleen, draining lymph nodes and thymus. Hence, we can hypothesise that even though Treg number in the thymus was reduced, peripheral Treg mediated tolerance tries to balance overshooting immune responses in the skin. Nevertheless, they greatly fail in doing so, suggesting a possibly non-solely-immunological basis of the skin inflammation by different – so far unknown – mechanisms. Otherwise, the SHARPIN deficiency induced inflammation might be just too severe for the even increased Treg population to control. There is definitively a necessity to follow up on these findings, analysing more mice and intensively focus on Treg

function in the skin. In addition, cytokine profiles should give a better idea on skin inflammatory nature.

A TRADD$^{E\text{-}KO}$ in CPDM mice is sufficient to rescue skin inflammation

By skin-conditionally targeting TRADD – a pivotal component for the TNF-α induced apoptosis signalling pathway – we anticipated to rescue hyper up regulation of programmed cell-death in CPDM mice. TRADD is an initial adaptor protein recruited to the TNF receptor complex (TNF-RC) upon TNF-α binding. Moreover, TRADD amongst other proteins dissociates from the TNF-RC, forms the DISC for apoptosis induction through caspase-8 and FADD. It was shown, that primary TRADD-KO MEF are unsusceptible for TNF-α induced programmed cell-death in contrast to CPDM MEF[122]. Remarkably, the TRADD$^{E\text{-}KO}$ in CPDM background completely rescued skin inflammation (Figure 16). This finding strongly favours our hypothesis of a cross talk between apoptosis and inflammation and that inflammation is actually driven by the hyper up regulation of apoptosis in SHARPIN deficient skin tissue. Therefore, SHARPIN's anti-apoptosis effects, through presumed binding and interaction to the DISC, in conjunction with down regulation of the Nf-κB pathway are crucial to maintain skin tissue homeostasis; and if missing, lead to cpdm phenotype. The link between controlled apoptotic cell-death and inflammation remains elusive. In the future, FADD/caspase-8 depletion in CPDM background will further address SHARPIN's precise function in the DISC. FADD itself was shown to protect against RIP3 mediated programmed necrosis in skin[130]. Therefore, to understand FADD in apoptosis, CPDM.FADD.RIP3$^{E\text{-}KO}$ triple knockout mice were generated and showed partial rescue and delay of skin inflammation (not published). In addition, in CPDM.RIP3$^{E\text{-}KO}$ animals the cpdm skin phenotype was alleviated; hence, necroptosis plays only a minor role for skin inflammation (not published) in CPDM mice.

Conclusion and future outlook

I showed that introducing a TRADD$^{E\text{-}KO}$ in CPDM mice rescued cpdm skin inflammation completely (Figure 16) but multi-organ phenotype was mostly unaffected (Figure 17). Blockage of TNF-α induced FADD-caspase-8 mediated apoptosis by target-

ing the TNF-RC and DISC component TRADD in an epidermis specific manner is sufficient to prevent skin inflammation in CPDM mice; hence, I conclude that SHARPIN deficiency induced hyper up regulation of apoptosis causes the inflammatory cpdm skin phenotype and can be rescued by blocking TNF-α induced apoptosis specifically by targeting the essential adaptor protein TRADD.

How a form of controlled cell-death can lead to inflammation remains an open debate. The exact mechanisms how SHARPIN interacts with the DISC and subsequent linear ubiquitination of FADD by LUBAC is yet to be found. In the future, assessing apoptosis induction in FADD KO cell lines and FADD depletion in CPDM MEF will give quantitative data showing that cytokine induced apoptosis induction works through FADD and the DISC. Furthermore, same experiment should be conducted with caspase-8 depleted CPDM MEF. The TNF-RC signals both for Nf-κB activation and apoptosis and are balanced in WT situation to maintain tissue homeostasis. I used the drug cycloheximide to block protein synthesis and thereby exclude Nf-κB's target gene expression. Introducing an overexpressed non-phosphorylatable IκBα variant in CPDM background will block Nf-κB in a less artificial way. CPDM.TRADD$^{E\text{-}KO}$ indicated partial rescue of the multi-organ phenotype (Figure 17) and to clarify these preliminary findings more mice have to be analysed and possible be crossed with a ubiquitously cre-expressing mice to generate CPDM.TRADD-KO mice.

References

1. Walsh, C. Posttranslational modifications of proteins: Expanding nature's inventory. (2006).
2. Hershko, A., Heller, H., Elias, S. & Ciechanover, A. Components of ubiquitin-protein ligase system. Resolution, affinity purification, and role in protein breakdown. *J. Biol. Chem.* **258,** 8206–8214 (1983).
3. Wilkinson, K. D., Urban, M. K. & Haas, A. L. Ubiquitin is the ATP-dependent proteolysis factor I of rabbit reticulocytes. *J. Biol. Chem.* **255,** 7529–7532 (1980).
4. Ciechanover, A., Heller, H., Elias, S., Haas, A. L. & Hershko, A. ATP-dependent conjugation of reticulocyte proteins with the polypeptide required for protein degradation. *Proceedings of the National Academy of Sciences* **77,** 1365–1368 (1980).
5. Komander, D. & Rape, M. The Ubiquitin Code. *Annu. Rev. Biochem.* **81,** 203–229 (2012).
6. Spence, J. *et al.* Cell cycle-regulated modification of the ribosome by a variant multiubiquitin chain. *Cell* **102,** 67–76 (2000).
7. King, R. W., Deshaies, R. J., Peters, J. M. & Kirschner, M. W. How proteolysis drives the cell cycle. *Science* **274,** 1652–1659 (1996).
8. Broemer, M. & Meier, P. Ubiquitin-mediated regulation of apoptosis. *Trends Cell Biol.* **19,** 130–140 (2009).
9. Sharp, P. M. & Li, W.-H. Ubiquitin genes as a paradigm of concerted evolution of tandem repeats. *J Mol Evol* **25,** 58–64 (1987).
10. Jentsch, S., Seufert, W. & Hauser, H. P. Genetic analysis of the ubiquitin system. *Biochim. Biophys. Acta* **1089,** 127–139 (1991).
11. Busch, H. & Goldknopf, I. L. Ubiquitin - protein conjugates. *Mol. Cell. Biochem.* **40,** 173–187 (1981).
12. Lange, O. F. *et al.* Recognition Dynamics Up to Microseconds Revealed from an RDC-Derived Ubiquitin Ensemble in Solution. *Science* **320,** 1471–1475 (2008).
13. Dikic, I., Wakatsuki, S. & Walters, K. J. Ubiquitin-binding domains - from structures to functions. *Nat. Rev. Mol. Cell Biol.* **10,** 659–671 (2009).
14. Haas, A. L. & Rose, I. A. The mechanism of ubiquitin activating enzyme. A kinetic and equilibrium analysis. *J. Biol. Chem.* **257,** 10329–10337 (1982).
15. Hochstrasser, M. Evolution and function of ubiquitin-like protein-conjugation systems. *Nat. Cell Biol.* **2,** E153–E157 (2000).
16. Ye, Y. & Rape, M. Building ubiquitin chains: E2 enzymes at work. *Nat. Rev. Mol. Cell Biol.* **10,** 755–764 (2009).
17. Pickart, C. M. & Eddins, M. J. Ubiquitin: structures, functions, mechanisms. *Biochim. Biophys. Acta* **1695,** 55–72 (2004).
18. Rieser, E., Cordier, S. M. & Walczak, H. Linear ubiquitination: a newly discovered regulator of cell signalling. *Trends in Biochemical Sciences* **38,** 94–102 (2013).
19. Komander, D., Clague, M. J. & Urbé, S. Breaking the chains: structure and function of the deubiquitinases. *Nat. Rev. Mol. Cell Biol.* **10,** 550–563 (2009).
20. Kirisako, T. *et al.* A ubiquitin ligase complex assembles linear polyubiquitin

chains. *The EMBO Journal* **25,** 4877–4887 (2006).
21. Ikeda, F., Crosetto, N. & Dikic, I. What Determines the Specificity and Outcomes of Ubiquitin Signaling? *Cell* **143,** 677–681 (2010).
22. Kulathu, Y. & Komander, D. Atypical ubiquitylation - the unexplored world of polyubiquitin beyond Lys48 and Lys63 linkages. *Nat. Rev. Mol. Cell Biol.* **13,** 508–523 (2012).
23. Scheffner, M., Nuber, U. & Huibregtse, J. M. Protein ubiquitination involving an E1-E2-E3 enzyme ubiquitin thioester cascade. *Nature* **373,** 81–83 (1995).
24. Lee, I. & Schindelin, H. Structural insights into E1-catalyzed ubiquitin activation and transfer to conjugating enzymes. *Cell* **134,** 268–278 (2008).
25. Huang, D. T. *et al.* Basis for a ubiquitin-like protein thioester switch toggling E1-E2 affinity. *Nature* **445,** 394–398 (2007).
26. Eletr, Z. M., Huang, D. T., Duda, D. M., Schulman, B. A. & Kuhlman, B. E2 conjugating enzymes must disengage from their E1 enzymes before E3-dependent ubiquitin and ubiquitin-like transfer. *Nat. Struct. Mol. Biol.* **12,** 933–934 (2005).
27. Joazeiro, C. A. & Weissman, A. M. RING finger proteins: mediators of ubiquitin ligase activity. *Cell* **102,** 549–552 (2000).
28. Scheffner, M., Huibregtse, J. M. & Howley, P. M. Identification of a human ubiquitin-conjugating enzyme that mediates the E6-AP-dependent ubiquitination of p53. *Proc. Natl. Acad. Sci. U.S.A.* **91,** 8797–8801 (1994).
29. Marín, I., Lucas, J. I., Gradilla, A.-C. & Ferrús, A. Parkin and relatives: the RBR family of ubiquitin ligases. *physiolgenomics.physiology.org*
30. Morett, E. & Bork, P. A novel transactivation domain in parkin. *Trends in Biochemical Sciences* **24,** 229–231 (1999).
31. VanDemark, A. Structural basis of ubiquitylation. *Current Opinion in Structural Biology* **12,** 822–830 (2002).
32. Kim, H. C. & Huibregtse, J. M. Polyubiquitination by HECT E3s and the determinants of chain type specificity. *Mol. Cell. Biol.* **29,** 3307–3318 (2009).
33. Pickart, C. M. Mechanisms underlying ubiquitination. *Annu. Rev. Biochem.* (2001).
34. Wenzel, D. M., Lissounov, A., Brzovic, P. S. & Klevit, R. E. UBCH7 reactivity profile reveals parkin and HHARI to be RING/HECT hybrids. *Nature* **474,** 105–108 (2011).
35. Stieglitz, B. *et al.* Structural basis for ligase-specific conjugation of linear ubiquitin chains by HOIP. *Nature* (2013). doi:10.1038/nature12638
36. Tokunaga, F. *et al.* Involvement of linear polyubiquitylation of NEMO in NF-κB activation. *Nat. Cell Biol.* **11,** 123–132 (2009).
37. Iwai, K. & Tokunaga, F. Linear polyubiquitination: a new regulator of NF-kappaB activation. *EMBO Rep* **10,** 706–713 (2009).
38. Ikeda, F. *et al.* SHARPIN forms a linear ubiquitin ligase complex regulating NF-κB activity and apoptosis. *Nature* **471,** 637–641 (2012).
39. Tanaka, K. *et al.* Familial Parkinson disease gene product, parkin, is a ubiquitin-protein ligase. *Nat Genet* **25,** 302–305 (2000).
40. Aguilera, M., Oliveros, M., Martínez-Padrón, M., Barbas, J. A. & Ferrús, A. Ariadne-

1: a vital Drosophila gene is required in development and defines a new conserved family of ring-finger proteins. *Genetics* **155,** 1231–1244 (2000).
41. Parelkar, S. S. *et al.* The Parkin-Like Human Homolog of Drosophila Ariadne-1 (HHARI) Can Induce Aggresome Formation in Mammalian Cells and Is Immunologically Detectable in Lewy Bodies. *J Mol Neurosci* **46,** 109–121 (2011).
42. Gerlach, B. *et al.* Linear ubiquitination prevents inflammation and regulates immune signalling. *Nature* **471,** 591–596 (2011).
43. Haas, T. L. *et al.* Recruitment of the linear ubiquitin chain assembly complex stabilizes the TNF-R1 signaling complex and is required for TNF-mediated gene induction. *Mol. Cell* **36,** 831–844 (2009).
44. Rahighi, S. *et al.* Specific recognition of linear ubiquitin chains by NEMO is important for NF-kappaB activation. *Cell* **136,** 1098–1109 (2009).
45. Tokunaga, F. *et al.* SHARPIN is a component of the NF-κB-activating linear ubiquitin chain assembly complex. *Nature* **471,** 633–636 (2011).
46. Xia, T. *et al.* Loss-of-function of SHARPIN causes an osteopenic phenotype in mice. *Endocr* **39,** 104–112 (2010).
47. Keusekotten, K. *et al.* OTULIN Antagonizes LUBAC Signaling by Specifically Hydrolyzing Met1-Linked Polyubiquitin. *Cell* **153,** 1312–1326 (2013).
48. Bromann, P. A., Weiner, J. A., Apel, E. D., Lewis, R. M. & Sanes, J. R. A putative ariadne-like E3 ubiquitin ligase (PAUL) that interacts with the muscle-specific kinase (MuSK). *Gene Expr. Patterns* **4,** 77–84 (2004).
49. Stieglitz, B., Morris-Davies, A. C., Koliopoulos, M. G., Christodoulou, E. & Rittinger, K. LUBAC synthesizes linear ubiquitin chains via a thioester intermediate. *EMBO Rep* **13,** 840–846 (2012).
50. Iwai, K. An ubiquitin ligase recognizing a protein oxidized by iron: implications for the turnover of oxidatively damaged proteins. *J. Biochem.* **134,** 175–182 (2003).
51. Ishikawa, H. *et al.* Involvement of heme regulatory motif in heme-mediated ubiquitination and degradation of IRP2. *Mol. Cell* **19,** 171–181 (2005).
52. Lim, S. *et al.* Sharpin, a novel postsynaptic density protein that directly interacts with the shank family of proteins. *Mol. Cell. Neurosci.* **17,** 385–397 (2001).
53. Stieglitz, B., Haire, L. F., Dikic, I. & Rittinger, K. Structural analysis of SHARPIN, a subunit of a large multi-protein E3 ubiquitin ligase, reveals a novel dimerization function for the pleckstrin homology superfold. *J. Biol. Chem.* **287,** 20823–20829 (2012).
54. Seymour, R. E. *et al.* Spontaneous mutations in the mouse Sharpin gene result in multiorgan inflammation, immune system dysregulation and dermatitis. *Genes Immun* **8,** 416–421 (2007).
55. Gijbels, M. J. *et al.* Pathogenesis of skin lesions in mice with chronic proliferative dermatitis (cpdm/cpdm). *Am. J. Pathol.* **148,** 941–950 (1996).
56. HogenEsch, H. *et al.* A spontaneous mutation characterized by chronic proliferative dermatitis in C57BL mice. *Am. J. Pathol.* **143,** 972–982 (1993).
57. Seymour, R., Shirley, B.-J., HogenEsch, H., Shultz, L. D. & Sundberg, J. P. Loss of

function of the mouse Sharpin gene results in Peyer's patch regression. *PLoS ONE* **8,** e55224 (2013).
58. Sen, R. & Baltimore, D. Inducibility of kappa immunoglobulin enhancer-binding protein Nf-kappa B by a posttranslational mechanism. *Cell* **47,** 921–928 (1986).
59. Siebenlist, U., Franzoso, G. & Brown, K. Structure, regulation and function of NF-kappa B. *Annu. Rev. Cell Biol.* **10,** 405–455 (1994).
60. Boyce, B. F., Yao, Z. & Xing, L. Functions of nuclear factor kappaB in bone. *Ann. N. Y. Acad. Sci.* **1192,** 367–375 (2010).
61. Napetschnig, J. & Wu, H. Molecular Basis of NF-κB Signaling. *Annu Rev Biophys* **42,** 443–468 (2013).
62. Han, Z., Boyle, D. L., Manning, A. M. & Firestein, G. S. AP-1 and NF-kappaB regulation in rheumatoid arthritis and murine collagen-induced arthritis. *Autoimmunity* **28,** 197–208 (1998).
63. Karin, M. NF-kappaB and cancer: mechanisms and targets. *Mol. Carcinog.* **45,** 355–361 (2006).
64. Jacobs, M. D. & Harrison, S. C. Structure of an IkappaBalpha/NF-kappaB complex. *Cell* **95,** 749–758 (1998).
65. Ghosh, S. & Baltimore, D. Activation in vitro of NF-kappa B by phosphorylation of its inhibitor I kappa B. *Nature* **344,** 678–682 (1990).
66. Baeuerle, P. A. The inducible transcription activator NF-κB: regulation by distinct protein subunits. *Biochimica et Biophysica Acta (BBA) - Reviews on Cancer* **1072,** 63–80 (1991).
67. Huguet, C., Crepieux, P. & Laudet, V. Rel/NF-kappa B transcription factors and I kappa B inhibitors: evolution from a unique common ancestor. *Oncogene* **15,** 2965–2974 (1997).
68. Gaur, U. & Aggarwal, B. B. Regulation of proliferation, survival and apoptosis by members of the TNF superfamily. *Biochemical Pharmacology* **66,** 1403–1408 (2003).
69. Hehlgans, T. & Pfeffer, K. The intriguing biology of the tumour necrosis factor/tumour necrosis factor receptor superfamily: players, rules and the games. *Immunology* **115,** 1–20 (2005).
70. Hsu, H., Huang, J., Shu, H.-B., Baichwal, V. & Goeddel, D. V. TNF-Dependent Recruitment of the Protein Kinase RIP to the TNF Receptor-1 Signaling Complex. *Immunity* **4,** 387–396 (1996).
71. Hsu, H., Xiong, J. & Goeddel, D. V. The TNF receptor 1-associated protein TRADD signals cell death and NF-kappa B activation. *Cell* **81,** 495–504 (1995).
72. Shu, H. B., Takeuchi, M. & Goeddel, D. V. The tumor necrosis factor receptor 2 signal transducers TRAF2 and c-IAP1 are components of the tumor necrosis factor receptor 1 signaling complex. *Proc. Natl. Acad. Sci. U.S.A.* **93,** 13973–13978 (1996).
73. Ea, C.-K., Deng, L., Xia, Z.-P., Pineda, G. & Chen, Z. J. Activation of IKK by TNFα Requires Site-Specific Ubiquitination of RIP1 and Polyubiquitin Binding by NEMO. *Mol. Cell* **22,** 245–257 (2006).

74. Locksley, R. M., Killeen, N. & Lenardo, M. J. The TNF and TNF Receptor Superfamilies. *Cell* **104,** 487–501 (2001).
75. Hayden, M. S. & Ghosh, S. Signaling to NF-κB. *genesdev.cshlp.org*
76. Pearson, G. *et al.* Mitogen-Activated Protein (MAP) Kinase Pathways: Regulation and Physiological Functions1. *http://dx.doi.org/10.1210/edrv.22.2.0428*
77. Micheau, O. & Tschopp, J. Induction of TNF receptor I-mediated apoptosis via two sequential signaling complexes. *Cell* **114,** 181–190 (2003).
78. Irmler, M. *et al.* Inhibition of death receptor signals by cellular FLIP. *Nature* **388,** 190–195 (1997).
79. Kreuz, S., Siegmund, D., Scheurich, P. & Wajant, H. NF-kappaB inducers upregulate cFLIP, a cycloheximide-sensitive inhibitor of death receptor signaling. *Mol. Cell. Biol.* **21,** 3964–3973 (2001).
80. Iwai, K. Diverse ubiquitin signaling in NF-κB activation. *Trends Cell Biol.* **22,** 355–364 (2012).
81. Chen, J. & Chen, Z. J. Regulation of NF-κB by ubiquitination. *Curr. Opin. Immunol.* **25,** 4–12 (2013).
82. Dynek, J. N. *et al.* c-IAP1 and UbcH5 promote K11-linked polyubiquitination of RIP1 in TNF signalling. *The EMBO Journal* **29,** 4198–4209 (2010).
83. Ivins, F. J. *et al.* NEMO oligomerization and its ubiquitin-binding properties. *Biochem. J.* **421,** 243–251 (2009).
84. Lo, Y.-C. *et al.* Structural basis for recognition of diubiquitins by NEMO. *Mol. Cell* **33,** 602–615 (2009).
85. Tokunaga, F. & Iwai, K. Linear ubiquitination: a novel NF-κB regulatory mechanism for inflammatory and immune responses by the LUBAC ubiquitin ligase complex. *Endocr. J.* **59,** 641–652 (2012).
86. Proksch, E., Brandner, J. M. & Jensen, J.-M. The skin: an indispensable barrier. *Exp. Dermatol.* **17,** 1063–1072 (2008).
87. Treuting, P. M., Dintzis, S. M., Frevert, C. W. & Montine, K. S. *Comparative Anatomy and Histology*. (Academic Press, 2012).
88. Madison, K. C. Barrier function of the skin: 'la raison d'être' of the epidermis. *J. Invest. Dermatol.* **121,** 231–241 (2003).
89. Houben, E., De Paepe, K. & Rogiers, V. A keratinocyte's course of life. *Skin Pharmacol Physiol* **20,** 122–132 (2007).
90. Reichert, U., Michel, S. & Schmidt, R. The cornified envelope: a key structure of terminally differentiating keratinocytes. *Molecular Biology of the Skin: …* (1993).
91. Paus, R. & Cotsarelis, G. The biology of hair follicles. *N. Engl. J. Med.* **341,** 491–497 (1999).
92. Wilke, K., Martin, A., Terstegen, L. & Biel, S. S. A short history of sweat gland biology. *Int J Cosmet Sci* **29,** 169–179 (2007).
93. Thody, A. J. & Shuster, S. Control and function of sebaceous glands. *Physiol. Rev.* **69,** 383–416 (1989).
94. Abbas, A. K., Lichtman, A. & Pillai, S. Basic immunology: functions and disorders of the immune system. (2012).

95. Fujiwara, N. & Kobayashi, K. Macrophages in Inflammation. *CDTIA* **4,** 281–286 (2005).
96. Spector, W. G. & Willoughby, D. A. The inflammatory response. *Bacteriological Reviews* **27,** 117 (1963).
97. Tak, P. P. & Firestein, G. S. NF-κB: a key role in inflammatory diseases. *J. Clin. Invest.* **107,** 7–11 (2001).
98. Coussens, L. M. & Werb, Z. Inflammation and cancer. *Nature* **420,** 860–867 (2002).
99. Gautier, E. L., Ivanov, S., Lesnik, P. & Randolph, G. J. Local apoptosis mediates clearance of macrophages from resolving inflammation in mice. *Blood* **122,** 2714–2722 (2013).
100. Opal, S. M. & DePalo, V. A. Anti-Inflammatory Cytokines. *CHEST* **117,** 1162–1172 (2000).
101. Moilanen, E. Two Faces of Inflammation: An Immunopharmacological View. *Basic Clin Pharmacol Toxicol* **114,** 2–6 (2013).
102. G Majno, I. J. Apoptosis, oncosis, and necrosis. An overview of cell death. *Am. J. Pathol.* **146,** 3 (1995).
103. Fuchs, Y. & Steller, H. Programmed Cell Death in Animal Development and Disease. *Cell* **147,** 742–758 (2011).
104. Jacobson, M. D. Programmed cell death: a missing link is found. *Trends Cell Biol.* **7,** 467–469 (1997).
105. Savill, J. & Fadok, V. Access : Corpse clearance defines the meaning of cell death : Nature. *Nature* **407,** 784–788 (2000).
106. Strasser, A., O'Connor, L. & Dixit, V. M. APOPTOSIS SIGNALING. *http://dx.doi.org/10.1146/annurev.biochem.69.1.217*
107. Cohen, G. M. Caspases: the executioners of apoptosis. *Biochem. J.* **326,** 1 (1997).
108. Earnshaw, W. C., Martins, L. M. & Kaufmann, S. H. MAMMALIAN CASPASES: Structure, Activation, Substrates, and Functions During Apoptosis. *Annu. Rev. Biochem.* **68,** 383–424 (1999).
109. Programmed Cell Death (Apoptosis). (2002).
110. Saelens, X. *et al.* Toxic proteins released from mitochondria in cell death. *Oncogene* **23,** 2861–2874 (2004).
111. Yuan, S. & Akey, C. W. Apoptosome Structure, Assembly, and Procaspase Activation. *Structure* **21,** 501–515 (2013).
112. Wallach, D., Kovalenko, A. V., Varfolomeev, E. E. & Boldin, M. P. Death-inducing functions of ligands of the tumor necrosis factor family: a Sanhedrin verdict. *Curr. Opin. Immunol.* **10,** 279–288 (1998).
113. MS, S. & Aj, F. Death and decoy receptors and p53-mediated apoptosis. **14,** – (2000).
114. Hayashida, M., Kawano, H., Nakano, T., Shiraki, K. & Suzuki, A. Cell death induction by CTL: perforin/granzyme B system dominantly acts for cell death induction in human hepatocellular carcinoma cells. *Proc. Soc. Exp. Biol. Med.* **225,** 143–150 (2000).

115. Deveraux, Q. L. & Reed, J. C. IAP family proteins—suppressors of apoptosis. *genesdev.cshlp.org*
116. Gross, A., McDonnell, J. M. & Korsmeyer, S. J. BCL-2 family members and the mitochondria in apoptosis. *genesdev.cshlp.org*
117. Safa, A. R. c-FLIP, a master anti-apoptotic regulator. *Exp. Oncol.* **34,** 176–184 (2012).
118. Liang, Y. & Sundberg, J. P. SHARPIN regulates mitochondria-dependent apoptosis in keratinocytes. *J. Dermatol. Sci.* **63,** 148–153 (2011).
119. HogenEsch, H., Janke, S., Boggess, D. & Sundberg, J. P. Absence of Peyer's patches and abnormal lymphoid architecture in chronic proliferative dermatitis (cpdm/cpdm) mice. *J. Immunol.* **162,** 3890–3896 (1999).
120. Yeh, W. C. *et al.* FADD: essential for embryo development and signaling from some, but not all, inducers of apoptosis. *Science* **279,** 1954–1958 (1998).
121. VARFOLOMEEV, E. Targeted Disruption of the Mouse Caspase 8 Gene Ablates Cell Death Induction by the TNF Receptors, Fas/Apo1, and DR3 and Is Lethal Prenatally. *Immunity* **9,** 267–276 (1998).
122. Ermolaeva, M. A. *et al.* Function of TRADD in tumor necrosis factor receptor 1 signaling and in TRIF-dependent inflammatory responses. *Nat Immunol* **9,** 1037–1046 (2008).
123. Pobezinskaya, Y. L. *et al.* The function of TRADD in signaling through tumor necrosis factor receptor 1 and TRIF-dependent Toll-like receptors. *Nat Immunol* **9,** 1047–1054 (2008).
124. www.varionostic.de/fileadmin/downloads/pyroprinciple_descr.pdf. *varionostic.de* at <http://www.varionostic.de/fileadmin/downloads/pyroprinciple_descr.pdf>
125. Michallet, M.-C. *et al.* TRADD Protein Is an Essential Component of the RIG-like Helicase Antiviral Pathway. *Immunity* **28,** 651–661 (2008).
126. Oshima, S. *et al.* ABIN-1 is a ubiquitin sensor that restricts cell death and sustains embryonic development. *Nature* **457,** 906–909 (2008).
127. Yilmaz, Z. B. RelB is required for Peyer's patch development: differential regulation of p52-RelB by lymphotoxin and TNF. *The EMBO Journal* **22,** 121–130 (2003).
128. Körner, H. *et al.* Distinct roles for lymphotoxin-α and tumor necrosis factor in organogenesis and spatial organization of lymphoid tissue. *Eur. J. Immunol.* **27,** 2600–2609 (1997).
129. Laboratories, J. CPDM phenotype overview. *jaxmice.jax.org* at <http://jaxmice.jax.org/strain/007599.html>
130. Bonnet, M. C. *et al.* The Adaptor Protein FADD Protects Epidermal Keratinocytes from Necroptosis In Vivo and Prevents Skin Inflammation. *Immunity* **35,** 572–582 (2011).

Annex

Summary

Ubiquitination is an essential post-translational modification, which is of fundamental importance in various cellular processes. Typical ubiquitin (Ub) chains – linked through their lysine (Lys) residues – have been intensively studied. In contrast, much less is known about methionine 1 'head-to-tail' linked linear-Ub (lin-Ub) chains. So far, only the E3 ligase complex 'LUBAC' is known to generate those 'atypical' Ub-chains. We and others showed that lin-Ub-chains are intrinsic for NF-κB activation and control of apoptosis. Furthermore, implications in skeletal development, tumourigenesis innate and adaptive immunity were found. Mice deficient for the regulatory LUBAC subunit SHARPIN (SHARPIN$^{cpdm/cpdm}$) suffer from the severe cpdm (chronic proliferative dermatistis in mice) multi-organ phenotype, characterised by overt skin inflammation, missing peyer's patch formation, splenomegaly and defective spleen germinal centre formation. Primary MEF isolated from these mice were defective in Nf-κB activation and intriguingly demonstrated to be hyper sensitive for TNF-α induced FADD-caspase-8 mediated apoptosis. Furthermore, we observed apoptosis marker cleaved caspase-3 positive cells by skin histology. Hence, we hypothesised a cross-talk between apoptosis and inflammation. Additional biochemical data suggested LUBAC-induced linear ubiquitination of a cell-death complex component FADD. TNF-α induced apoptosis revealed to be blocked in mice genetically ablated for the adaptor protein TRADD (TNF receptor 1 associated protein with death domain) whereas FADD/caspase-8 knockout mice were embryonic lethal. Here I show that an epidermis specific TRADD knockout (TRADD$^{E\text{-}KO}$) in SHARPIN$^{cpdm/cpdm}$ background rescues skin inflammation. H&E staining, antibody specific immunohistochemistry for macrophages and apoptotic cells of skin sections revealed a complete recovery to wild type skin architecture in SHARPIN$^{cpdm/cpdm}$.TRADD$^{E\text{-}KO}$ double knockout animals. System-wide cpdm phenotypes remained unaffected.

Zusammenfassung

Ubiquitinierung von Proteinen ist eine essentielle posttranslationelle Modifikation, die an einer Vielzahl von zellulären Prozessen von integraler Bedeutung ist. Typische Ub-Ketten, untereinander verlinkt über Lysine (Lys), wurden intensiv in der Molekularbiologie erforscht. Im Gegensatz dazu ist über atypische linear Ubiqutinketten, die durch eine Verlinkung via Methionin 1 charakterisiert sind, relativ wenig bekannt. Ub Ligase-Komplex „LUBAC" ist bisher die einzige identifizierte Enzymkomplex der im Stande ist, diese lineare-Ubiquitinketten, zu generieren. Wir und Andere haben bereits gezeigt, dass von LUBAC erzeugte lineare Ubiquitinketten in verschiedenen Signalwegen, darunter der TNF-alpha induzierte Nf-κB- und Apoptose-Signalweg, elementar sind. Ein für die regulatorische LUBAC-Untereinheit SHARPIN defizientes Mausmodell (SHARPIN$^{cpdm/cpdm}$) zeichnet sich durch offensichtliche Hautentzünungserscheinungen, bezeichnet als chronic proliferative dermatistis in mice (cpdm), als auch über systemweite Defekte in Organen wie Lunge und Milz, als auch in sekundären immunologischen Geweben aus. SHARPIN$^{cpdm/cpdm}$ primär isolierte embryonale Fibroblasten haben reduzierte Nf-κB-Aktivität und zeigen interessanterweise hochregulierte Apoptose in Keratinocyten nach Behandlung mit TNF-alpha *in vitro*. Deshalb hypothetisieren wir einen Zusammenhang zwischen Apoptose und Entzündung in den Keratinozyten, welcher durch zusätzliche Biochemiedaten, die LUBAC spezifische Ubiquitinierung der Apoptose-Signalweg Komponente FADD, untermauert wird. Hier zeige ich, dass durch Kreuzen von SHARPIN$^{cpdm/cpdm}$ Mäusen mit einer epidermis-spezifischen TRADD (TNF receptor 1 associated protein with death domain), Knock-Out Maus (TRADD^{E-KO}), eines für TNF-alpha vermittelten Apoptose unabdingbarem Adaptorprotein, gerettet wird. Hautgewebeschnitte, welche durch Standard H&E als auch mit Antikörper spezifisch für Zelltodmarker sowie Makrophagen gefärbt wurde, zeigen eine komplette Wiederherstellung der Wildtyp-Situation der Haut in SHARPIN$^{cpdm/cpdm}$.TRADD^{E-KO} Doppel-KO-Mäusen. Die systemweiten Defekte des SHARPIN$^{cpdm/cpdm}$ Phänotypen bestehen unverändert weiter.

Curriculum Vitae

PERSONAL INFORMATION

Name	**LUTZMAYER STEFAN**
Nationality	AUSTRIA
Date of birth	23/06/1987

SCIENTIFIC EXPERIENCE

• Dates (from – to)	**JULY 2010 – OCTOBER 2010**
• Name and address of employer	University of Vienna Department of Biochemistry Group WICHE | Advisor Mag. Dr. Selma Osmanagic-Myers
• Type of business or sector	Academic Research
• Occupation or position held	Bachelor student
• Dates (from – to)	**JANUARY 2012 – MARCH 2012**
• Name and address of employer	Veterinary University of Vienna Institute of Pharmacology and Toxicology Group SEXL | Advisor Mag. Angelika Berger
• Type of business or sector	Academic Research
• Occupation or position held	Internship
• Dates (from – to)	**SEPTEMBER 2012 – OCTOBER 2013**
• Name and address of employer	Institute of Molecular Biotechnology of the Austrian Academy of Science Group IKEDA | Advisor Fumiyo Ikeda, PhD
• Type of business or sector	Academic Research
• Occupation or position held	Master student

EDUCATION

• Dates (from – to)	**2007 – 2011**
• Name and type of organisation providing education and training	University of Vienna
• Principal subjects/occupational skills covered	Bachelor Study in the field of Biology with emphasis on Molecular Biology
• Title of qualification awarded	Bachelor of Science
• Dates (from – to)	**2011 – PRESENT**
• Name and type of organisation providing education and training	University of Vienna
• Principal subjects/occupational skills covered	Master Study in the field Molecular Biology with emphasis on Cell Biology and Biochemistry
• Target Degree	Master of Science